MATERIALS CHEMISTRY
FRONTIERS

REVIEW

Cite this: *Mater. Chem. Front.*, 2020, **4**, 12

pH-Controlled motions in mechanically interlocked molecules

He-Ye Zhou,[ab] Ying Han*[ab] and Chuan-Feng Chen *[ab]

Received 28th August 2019,
Accepted 30th September 2019

DOI: 10.1039/c9qm00546c

rsc.li/frontiers-materials

Mechanically interlocked molecules (MIMs), especially rotaxanes and catenanes, allow large-amplitude movement at the molecular level, making them the perfect prototypes for artificial molecular switches and machines. By applying external stimuli, the noncovalent interactions between their subcomponents can be interrupted and formed reversibly, leading to mechanical motions. Among various stimuli, pH stimulation is one of the most powerful and commonly used means of controlling motions by acids and bases. In this review, we summarize the pH-controlled mechanical motions including translocation in rotaxanes, circumrotation in catenanes and other kinds of motion in more sophisticated mechanomolecules, and discuss their operating mechanisms. In addition, we present several more recent developments of alternative stimuli for pH responsive motions.

1. Introduction

Mechanically interlocked molecules (MIMs),[1] typically rotaxanes, catenanes and knots, have attracted widespread attention, not only because of their charming topological structures,[2] but also as a consequence of their ability to undergo controllable motion between their subcomponents.[3] At first, introducing a mechanical bond into a molecule makes it possible to change the co-conformations of MIMs under external stimuli. Then, the interlocked structures can constrain the magnitude of the subcomponents' movement by an entanglement in three-dimensional space. As a result, the MIMs which contain two or more different recognition sites can provide the perfect prototypes for the design and synthesis of artificial molecular switches and machines.[4] This research field was highlighted by the Nobel prize in 2016 for Chemistry to Stoddart and Sauvage, alongside Feringa.[5] Rotaxanes[6] are described as compounds that comprise a dumbbell-shaped guest threaded through the cavity of a ring. If it is properly designed, translational motion of the ring along its associated dumbbell can be triggered under proper stimulation (Fig. 1a). Catenanes,[7] which comprise two or more interlocking ring-shaped component parts, can interconvert between co-conformations by circumrotational motion of a small ring with respect to a larger one (Fig. 1b). Taking advantage of the interconversion between different co-conformations of MIMs, more diverse and sophisticated kinds of motion have been successfully fulfilled at the molecular level.[8]

[a] *Beijing National Laboratory for Molecular Sciences, CAS Key Laboratory of Molecular Recognition and Function, Institute of Chemistry, Chinese Academy of Sciences, Beijing 100190, China. E-mail: cchen@iccas.ac.cn, hanying463@iccas.ac.cn*
[b] *University of Chinese Academy of Sciences, Beijing 100049, China*

He-Ye Zhou

He-Ye Zhou received his BS degree from Xiangtan University. In 2016, he joined the laboratory of Prof. Chuan-Feng Chen at Institute of Chemistry, Chinese Academy of Sciences (ICCAS) to pursue his PhD in chemistry. His current research interest is the construction and applications of mechanically interlocked molecules based on triptycene-derived macrocyclic hosts.

Ying Han

Ying Han received her BS from Capital Normal University (CNU) in 2007, MS degree from CNU in 2010 under the guidance of Prof. Sheng-Li Cao, and PhD in 2013 from ICCAS under the guidance of Prof. Chuan-Feng Chen. She is now working as an associate professor at ICCAS. Her current research interests are supramolecular chemistry based on new synthetic hosts and molecular machines.

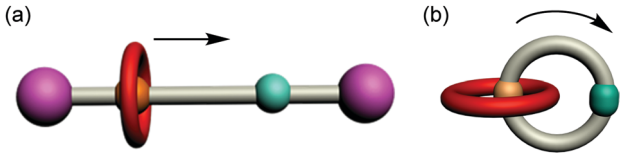

Fig. 1 Cartoon illustrations of mechanical motions: (a) translocation in typical [2]rotaxanes; (b) circumrotation in typical [2]catenanes.

The external stimuli, including chemical,[9] photochemical,[10] and electrochemical[11] stimuli, are considered as an energy input to regulate the co-conformations of the MIMs, generating controllable motions. Among various external stimuli, pH stimulation is considered as one of the most convenient and efficient methods to regulate the subcomponents' motion by readily available acids and bases, which belongs to chemical stimulation.[12] Until recently, various types of macrocyclic hosts (crown ethers, cucurbiturils, tetracationic cyclophanes, amide-based macrocycles, calixarenes, *etc.*) have been incorporated in MIMs that perform pH-triggered motions. These pH-responsive systems have two obvious features: (i) MIMs (host or guest) usually contain reactive donor atoms (*e.g.* nitrogen and oxygen atoms), which are easily protonated and deprotonated with acids and bases; (ii) non-covalent interactions, particularly, hydrogen bonding, hydrophobic effects, and electrostatic interactions are very sensitive to pH variation. Therefore, acid/base has been one of the most useful stimuli for controllable motions in MIMs.

We herein present an overall review of pH-responsive motions in MIMs. In the first section, we focus on operating translational motions in rotaxane architectures based on different recognition motifs. Then, the circumrotational motions in typical [2]catenanes are discussed. Next, we turn our attention to the motions beyond linear translation and circumrotation in more sophisticated mechanomolecules. Finally, we describe the recent progress made on actuating pH-responsive motions with alternative stimuli instead of acids and bases. This review will not discuss pH-switchable association and disassociation between host and guest.

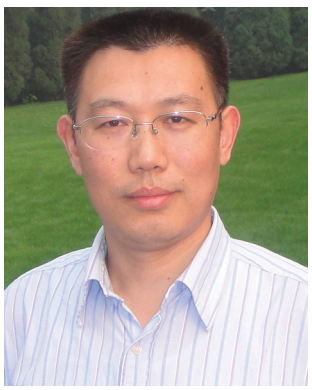

Chuan-Feng Chen

Chuan-Feng Chen has been working as a full professor of organic chemistry at Institute of Chemistry, Chinese Academy of Sciences since 2001. His current research interests include supramolecular chemistry based on synthetic macrocyclic hosts, chiral organic light-emitting materials and helicene chemistry.

2. Operating translocation in rotaxanes

Rotaxanes, the most studied interlocked molecules, have been a versatile platform to construct stimuli-responsive molecular shuttles. Within rotaxane architectures, the associated thread usually contains two or more recognition sites with different binding affinities for the rings. By weakening or increasing the affinity of the binding sites under external stimuli, the macrocycle can be driven to shuttle from one site to another site. When there exists a protonated ammonium, pyridinium or phenolic unit in MIMs, the association and disassociation process is readily controlled by acids and bases. The addition or removal of protons in a ring or thread might change the existing hydrogen-bonding, electrostatic interactions or hydrophobic effect dramatically, resulting in mechanical movement. In this section, we focus on the acid/base-controlled translocation in rotaxanes. Different recognition motifs based on various macrocyclic hosts and their operating mechanism will be discussed.

2.1 pH-Controlled translocation based on cucurbiturils

Cucurbit[*n*]urils (CB[*n*]),[13] prepared by condensation of glycoluril with formaldehyde in acidic medium, are an important family of macrocyclic compounds in supramolecular and mechanically bonded systems. They are well known for their extraordinary affinity towards alkanediammoniums in water driven by the hydrophobic effect and ion–dipole interactions between the ammoniums and the polar carbonyl groups at the portals of CB[*n*]. Accordingly, host–guest binding between CBs and ammoniums is strongly pH-dependent, which paves the way for constructing pH-controllable molecular motions. In this respect, pioneering works of pH-driven shuttling were performed in 1990 by Mock[14] and Kim.[15] A bistable [2]rotaxane $\mathbf{1H_2}^{2+}$ with electrostatic bipyridinium ($BIPY^{2+}$) stoppers was designed and synthesized.[16] The switchable translational motion of the CB[6] was driven by pH variation (Fig. 2). Under the acidic condition, the CB[6] resides exclusively on the central protonated diaminobutane unit promoted by hydrophobic effects and hydrogen-bonding interactions. Upon deprotonation of the butanediammonium in $\mathbf{1H_2}^{2+}$ by diisopropylethylamine (DIEA), the CB[6] ring moves to one of the peripheral bis(pyridinium) hexane units in **1**. But the reverse process requires hydrochloric acid plus thermal activation.

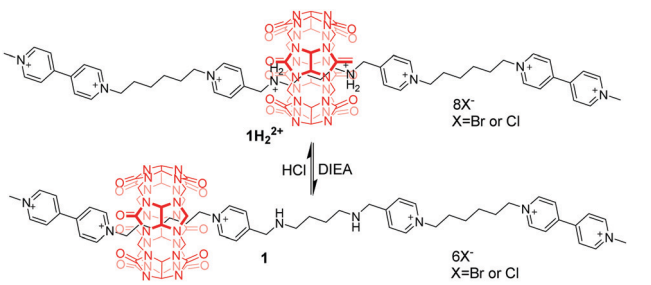

Fig. 2 pH-Controlled CB[6]-based [2]rotaxane **1** with electrostatic $BIPY^{2+}$ stoppers.

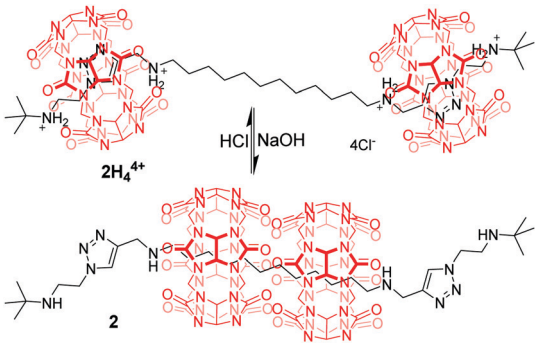

Fig. 3 Tuncel's acid/base switchable palindromic [3]rotaxane **2**.

A few examples of pH-dependent [3]rotaxanes based on CB[6] have been reported by Tuncel.[17] [3]rotaxane $\mathbf{2H_4}^{4+}$ (Fig. 3) was prepared by CB[6]-catalyzed 1,3-dipolar cycloaddition reaction, which is composed of two CB[6] rings, each encircling triazole-bis(ammonium) units near the termini of the *tert*-butyl group. When NaOH was used to neutralize the ammonium groups, two CB[6] rings moved to the more hydrophobic dodecamethylene spacer. Conversely, the rings return to the triazole units in **2** after the amines have been reprotonated with HCl. Similar motifs were also incorporated into a tetrapodal [5]rotaxane to give a pH-driven radial translocation.[18] Based on the similar working mechanism, CB[7] was also used for the construction of pH-controlled motions.[19]

2.2 pH-Controlled translocation based on tetracationic cyclophanes

Tetracationic cyclophanes,[20] which consist of two π-electron-deficient 4,4′-bipyridinium units, are capable of strongly binding with π-electron-rich guests. One of the most famous cyclophanes is cyclobis(paraquat-*p*-phenylene) ($\mathrm{CBPQT^{4+}}$), developed by the group of Stoddart,[21] which is known as the "blue box". Taking advantage of the $\mathrm{CBPQT^{4+}}$, the molecular shuttle was achieved based on π-associated donor–acceptor interactions.[22] The [2]rotaxane **3** contains the $\mathrm{CBPQT^{4+}}$ and a linear molecule axle with benzidine and biphenol recognition sites (Fig. 4). Under neutral pH and at 229 K, the macrocycle mainly located at the benzidine position in the dumbbell, because the binding affinity of $\mathrm{CBPQT^{4+}}$ for the benzidine derivative was about 10 times greater than that for the corresponding biphenol derivative. Addition of excess trifluoroacetic acid (TFA) to pronate benzidine resulted in macrocyclic translocation to the biphenol station owing to electrostatic repulsion. Subsequently TFA-induced shuttling motion could be fully reversed by neutralization of TFA with pyridine. Another important feature was that this translational motion could also be triggered by electrochemical means. Since Stoddart's invention of the switchable molecular shuttle, chemists have used molecular switching to perform a variety of "on"/"off" tasks with synthetic MIMs.

2.3 pH-Controlled translocation based on crown ethers

Crown ethers and their derivatives have been continuingly popular for the fabrication of pH-responsive MIMs. They are of versatile binding ability towards an enormous variety of organic guests, especially dialkylammonium ions, based on hydrogen-bond interactions and electrostatic interaction. These interactions can be destroyed simply by removing the hydrogen linked to the nitrogen in the guest molecules with appropriate base. Hence, lots of pH-responsive crown ether-based MIMs have been reported in the last few decades.

Among the crown ethers and their derivatives, dibenzo-24-crown-8 (DB24C8) is the most commonly designed and synthesized pH-responsive molecular switch and machine. Different recognition sites for DB24C8 have been explored to construct pH-switchable rotaxanes. Diallkylammomium is usually employed as a reversible control unit and another permanent cation as a second recognition site. This strategy has generated various examples owing to the discovery of novel recognition stations for DB24C8. Early research was founded by Stoddart[23] that [2]rotaxane containing a dibenzylammonium unit ($\mathrm{R_2NH^{2+}}$) and bipyridinium unit ($\mathrm{BIPY^{2+}}$) can be switched by acid/base. The key to this design lies in the fact that DB24C8 binds $\mathrm{R_2NH^{2+}}$ more strongly than $\mathrm{BIPY^{2+}}$. Thus, the DB24C8 ring encircles the $\mathrm{R_2NH^{2+}}$ site almost exclusively in $\mathbf{4H}^+$ (Fig. 5a), whereas conversion to the corresponding amine 4 with i-$\mathrm{Pr_2NEt}$ causes the ring to shuttle to the $\mathrm{BIPY^{2+}}$ unit. The rotaxane $\mathbf{4H}^+$ can be easily regenerated by simply reprotonating the amine with TFA. Subsequently, a pH-controlled molecular switch $\mathbf{5H}^+$ (Fig. 5b) was developed referring to the mechanism behind the operation of $\mathbf{4H}^+$.[24] The stopper adjacent to the $\mathrm{R_2NH^{2+}}$ center was replaced with anthracene as a fluorophore. This modification made it possible to investigate the detailed kinetics of the shuttling process by using the stopped-flow spectroscopic technique.[25] In 2016,

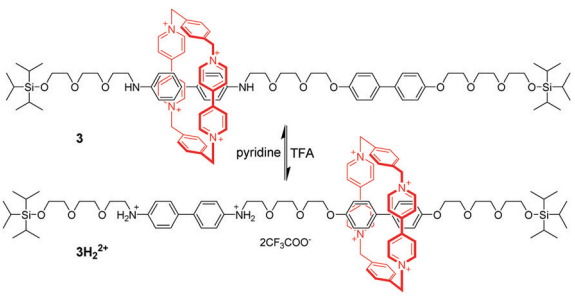

Fig. 4 pH-Switchable molecular shuttle **3** driven by π-associated donor–acceptor interactions.

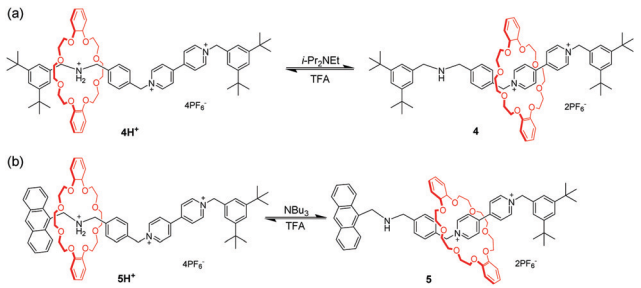

Fig. 5 Acid/base-driven molecular shuttles **4** and **5** containing a dibenzylammonium unit and bipyridinium unit.

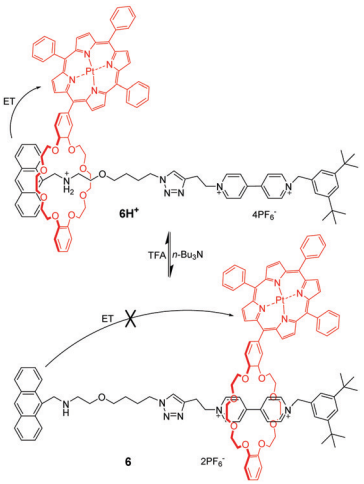

Fig. 6 [2]Rotaxane **6** with pH-switchable room temperature phosphorescence.

Ma and co-workers[26] introduced this operating mechanism into a molecular shuttle whose shuttling was encoded by room temperature phosphorescence (RTP) signals. As shown in Fig. 6, [2]rotaxane **6** comprises a Pt(II) porphyrin-containing DB24C8 threaded onto two different recognition sites and the anthracene moiety as a one terminal stopper. In the protonated state, the macrocycle was located on the R_2NH^{2+} site close to the anthracene unit, and the porphyrin unit exhibited strong RTP emission due to the distance-dependent energy transfer between the anthracene and the porphyrin. However, deprotonation of the R_2NH^{2+} unit could engender the displacement of the macrocycle to the $BIPY^{2+}$ station, and its RTP emission dramatically decreased.

Since Coutrot's report in 2008,[27] *N*-methyltriazolium has become another popular molecular station for the crown ether, which is easily generated *via* methylation of the triazole formed during a copper(I)-catalyzed azide-alkene cycloaddition (CuAAC) 'click' stoppering reaction in a high yield. The triazolium ion has a much poorer affinity for the DB24C8 than the ammonium, which makes triazoliums an ideal second molecular station. As a consequence, in the bistable [2]rotaxane $\mathbf{7H^+}$, the DB24C8 ring initially resides around the anilinium site (Fig. 7). However, deprotonation of the ammonium station triggers the shuttling motion of the crown ether toward the triazolium station. This process can be willingly reset by addition of acid. From then on, a number of MIMs have adopted the trizolium motif to develop pH-sensitive molecular machines.[28] For example, functionalized [2]rotaxanes with pH-switchable fluorescent outputs have been achieved.[29] Besides, triazolium-containing [3]rotaxane, [4]rotaxane and [5]rotaxane molecular machines were reported by several

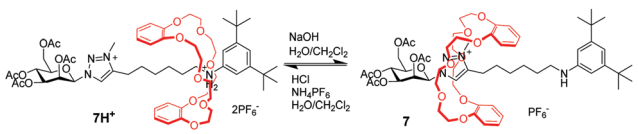

Fig. 7 pH-Switchable [2]rotaxane adopting a triazolium moiety.

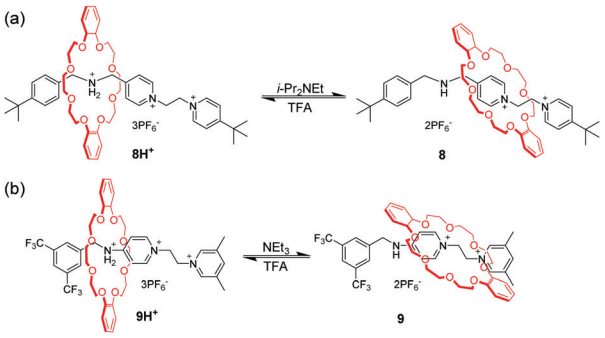

Fig. 8 pH-Switchable [2]rotaxane utilizing BPE^{2+} as a second recognition site.

researchers, including Liu,[30] Li,[31] Tian,[32] Qu[33] and so on.[34] In recent years, Leigh *et al.* creatively used a crown ether and triazolium motif to prepare an appealing rotaxane-based switchable organocatalyst.[35]

Loeb *et al.*[36] found that the 1,2-bis(pyridinium)ethane dication (BPE^{2+}) could also serve as a binding site for DB24C8. Subsequently, by utilizing BPE^{2+} as a second recognition site, acid/base-controllable molecular shuttles containing DB24C8 were constructed by Stoddart and Loeb (Fig. 8).[37] The benzimidazolium ion is another common recognition template for developing MIMs with crown ethers due to their rigid core and pH responsiveness. However, the interaction of DB24C8 with either the imidazolium or phenylbenzimidazolium cation is quite weak. Hence, Loeb and co-workers developed a new T-shaped benzimidazolium cation which could severe as an efficient template for the formation of [2]pseudorotaxanes with crown ethers.[38] This templating motif was incorporated into acid–base controllable molecular shuttles. [2]Rotaxane $\mathbf{10H_2^{2+}}$ containing two benzimidazole recognition sites on a single axle but only a single macrocyclic wheel could function as a molecular shuttle by acid–base chemistry (Fig. 9).[39] The neutral form of the molecular shuttle **10** shows an extremely rapid shuttling due to lower barrier. Addition of one equivalent of acid to give $\mathbf{10H^+}$ arrests the shuttling due to a protonated site which is complexed and a neutral site which is uncomplexed. Diprotonation produces $\mathbf{10H_2^{2+}}$ containing two recognition sites and the shuttling is resumed but at a much lower rate due to an increased barrier to translational motion. More interestingly, this molecular shuttle for the first time was embedded into a metal–organic framework (MOF) material allowing rapid shuttling motions in its skeletal framework.[40] In addition, Loeb's group reported acid–base switchable [2]- and [3]rotaxane molecular shuttles by combining 1,2-bis(pyridinium)ethane and benzimidazolium recognition motifs.[41]

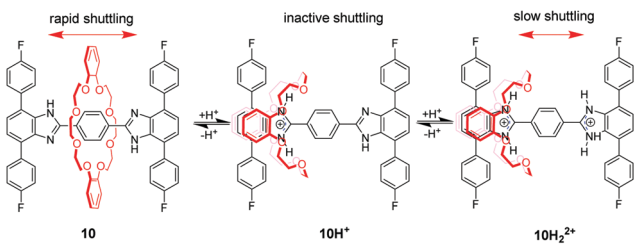

Fig. 9 Rigid H-shaped [2]rotaxane shuttle **10**.

2.4 pH-Controlled translocation based on benzylic amide macrocycles

Amide-based macrocycles also bind neutral guests through hydrogen bonding, which have been effectively used for pH-triggered molecular shuttles. The first example of pH-switchable shuttling involved anion recognition of a benzylic amide macrocycle by Leigh's group.[42] [2]Rotaxane **11H** contains a benzylic amide ring threaded onto an axle incorporating two potential hydrogen bonding stations (Fig. 10). One of them is a coumaric amide chromophore with a phenolic group that can be deprotonated by various bases to afford an oxyanion. In the neutral form, the macrocycle resides preferentially on the succinamide station in DMF. Under basic conditions, the macrocycle shuttles away to participate in strong hydrogen bonding interactions with the corresponding phenolic oxyanion of $\mathbf{11}^{-}$. Subsequent addition of TFA reprotonates the phenolic group and returns the ring to the succinamide location.

Another of Leigh's example of pH-triggered shuttling motion was based on a Pd(II)-complexed benzylic amide macrocycle.[43] Pyridine (PY) and dimethylaminopyridine (DMAP) were chosen as recognition sites to form a Pd-complex with an amide macrocycle. And DMAP is a stronger base which coordinates preferentially to Pd(II) ion ensconced in the macrocycle in **12** (Fig. 11). The addition of an equivalent of *p*-toluenesulfonic acid (TsOH) protonates the DMAP unit selectively, thus leading to migration of the macrocycle to the PY site. As a consequence,

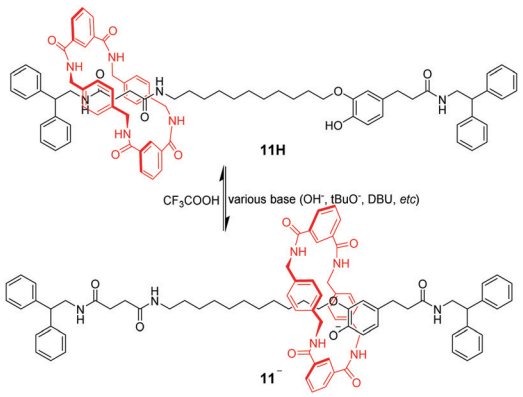

Fig. 10 pH-Switchable shuttling involved anion recognition.

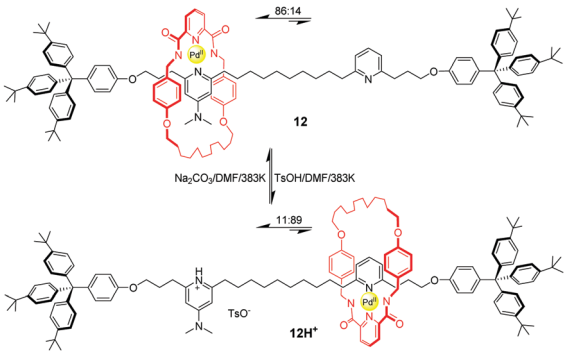

Fig. 11 pH-Switchable palladium-complexed molecular shuttle **12**.

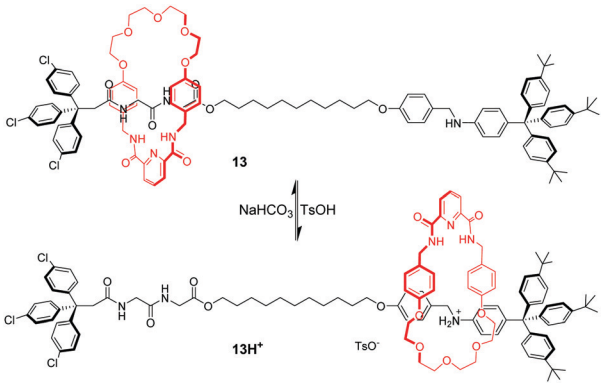

Fig. 12 pH-Controlled molecular shuttle **13** based on a hybrid polyether/amide macrocycle.

the ratios of translational isomer **12** and $\mathbf{12H}^{+}$ could be actuated from 86 : 14 to 11 : 89 by acid–base chemistry. Later, they developed a second generation of this molecular shuttle, which shows significantly increased rates of shuttling and improved co-conformational bias.[44]

By integrating amide–amide hydrogen bonding and crown ether–ammonium cation interactions, a pH-switchable molecular shuttle with dual binding mode was achieved.[45] As illustrated in Fig. 12, the thread component of rotaxane **13** contains glycylglycine (GlyGly) and anilinium as recognition sites and an isophthalamide group and polyether chain in the macrocycle. The ring encircles a dipeptide unit stabilized by amide–amide hydrogen bonds in the neutral form. When aniline is protonated with TsOH, polyether–ammonium cation interactions dominate and the macrocycle migrates to the anilinium station in $\mathbf{13H}^{+}$. By using the same principle, several pH-controlled molecular shuttles based on this hybrid polyether/amide macrocycle were also developed by Li,[46] Chiu[47] and Wang.[48]

Lüning and co-workers[49] also reported a pH-induced molecular shuttle using pyridine-modified benzylic amide macrocycle. The shuttling process can be operated by protonation/deprotonation of the ring. In [2]rotaxane **14** in Fig. 13, the benzylic amide ring initially resides at one end of the dumbbell where two supramolecular interactions favor this orientation: hydrogen bonds and donor–acceptor interactions with amide and pyridinium units adjacent to the stopper. After the protonation of ring's

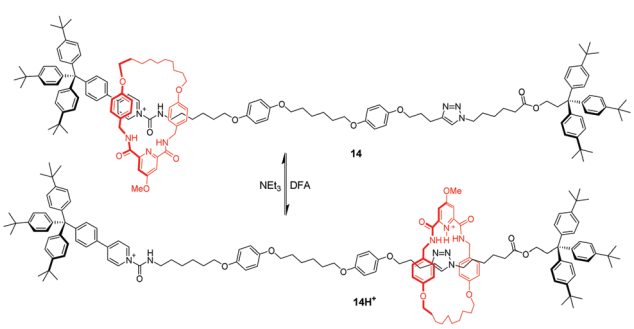

Fig. 13 pH-Induced molecular shuttle **14** using a pyridine-modified benzylic amide macrocycle.

pyridyl group with difluoroacetic acid (DFA), the macrocycle shuttles to the triazole station as a result of electrostatic repulsion and an increased propensity to interact with the triazole units.

2.5 pH-Controlled rotaxanes based on calix[6]arene

Calix[6]arene (CA6), with an electron-rich cavity, tends to bind protonated secondary ammonium or tertiary ammonium, which can be efficiently controlled by acid/base. Neri and co-workers[50] demonstrated the first example of calix[6]arene-based molecular shuttles. As shown in Fig. 14, a dibenzylammonium-containing axle molecule thread into the cavity of a calix[6]arene derivative in the [2]rotaxanes **15aH**$^+$ and **15bH**$^+$, which differ only in their methoxyl and *n*-hexyloxyl group appended at the calix[6]arene lower rim. And the macrocycle surrounds exclusively the dibenzylammonium site in a cone conformation for the formation of hydrogen bonds between its OR groups and ammonium. Upon deprotonation of the ammonium with phosphazene base P$_1$^{t}Bu (*N*-*tert*-butyl-*N*′,*N*′,*N*″,*N*″,*N*‴,*N*‴-hexamethylphosphorimidic triamide), the biased shuttling motion in neutral [2]rotaxane was observed to give two translational isomers, **15L** and **15U**, in which the alkoxy moieties at the lower rim or the *tert*-butyl groups at the upper rim are facing the trityl stopper, respectively. And the rate of the two isomers of **15a** is much more biased (K = 32) than that (K = 1.5) of **15b**, which may be ascribed to the formation of stronger hydrogen-bonding interactions in **15a** with the urethane group linked to the stoppers. More interestingly, the CA6 ring of **15a** can undergo a cone-to-cone inversion of the macrocycle *via* through-the-annulus passage of the small OMe group (Fig. 15).

Based on an analogous motif, Neri's group[51] also reported a pH-controllable [3]rotaxane to investigate their shuttling behaviour. They prepared methoxyl-containing [3]rotaxane (H,H)-**16H**$^+$ (Fig. 16) with head-to-head stereosequence of the two calix[6]arenes and tail-to-tail [3]rotaxane (T,T)-**17H**$^+$ (Fig. 17). When neutralizing the (H,H)-**16H**$^+$ and (T,T)-**17H**$^+$, the two macrocycles move from alkylbenzylammonium stations to new positions where aliphatic chains are inside the cavity of CA6. Simultaneously, the CA6 rings can experience cone-to-cone inversion to give three possible translational isomers, which feature as head-to-head (H,H), head-to-tail (H,T), and tail-to-tail (T,T). As a result,

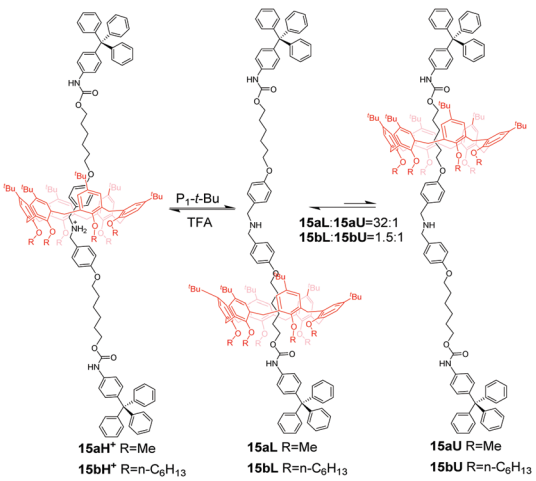

Fig. 14 pH-Induced molecular shuttle **15** based on calix[6]arene.

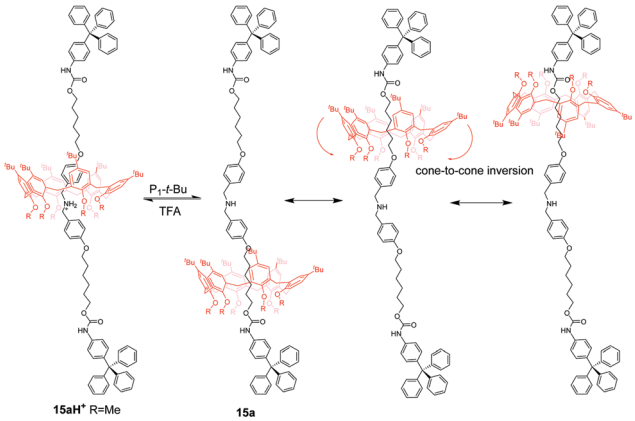

Fig. 15 Combined translocation/inversion motion of the calix[6]-wheel in [2]rotaxane **15a**.

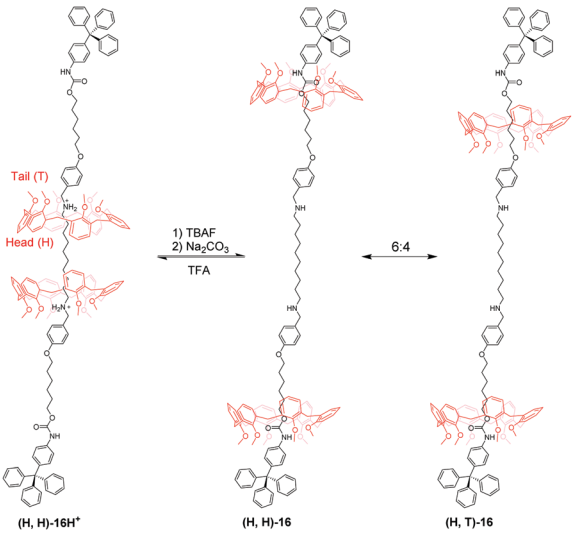

Fig. 16 pH-Controlled calix[6]arene-based [3]rotaxane **16**.

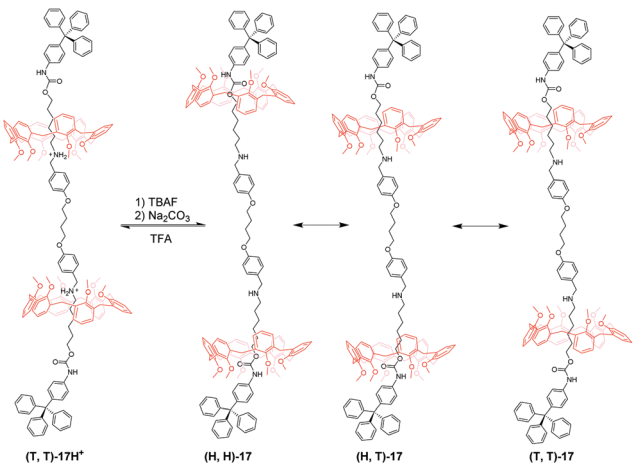

Fig. 17 pH-Controlled calix[6]arene-based [3]rotaxane **17**.

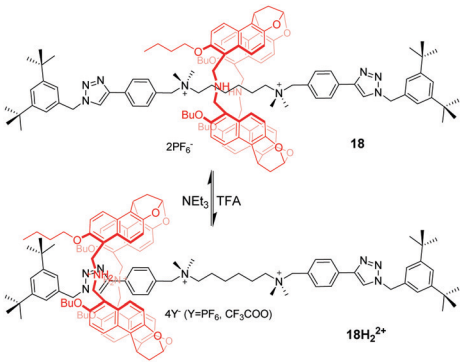

Fig. 18 Directional shuttling in naphthotube-based rotaxane.

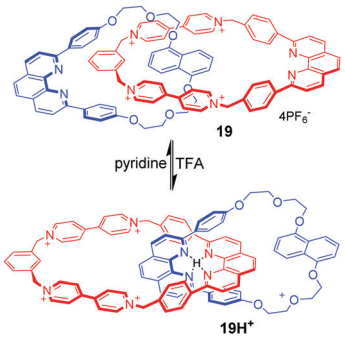

Fig. 19 pH-Responsive hybrid [2]catenane **19**.

only two isomers were observed in **16**, including (H,H)-**16** and (H,T)-**16** with a ratio of 6 : 4. But in **17**, there exist (H,H)-**17**, (H,T)-**17**, and (T,T)-**17** in a 55 : 25 : 20 ratio. Finally, the acidic treatment of neutral rotaxane fully restored the original state.

2.6 Directional shuttling in naphthotube-based rotaxane

Jiang *et al.*[52] reported naphthol-based macrocyclic receptors, namely naphthotubes, with two secondary amine groups in their backbones. Thus, two different binding properties of this macrocycle can be expected as its electron-rich cavity can be switched to positively charged by adding acid. In this way, they designed and synthesized a molecular shuttle **18** in which the macrocycle locates around the centre di(quaternary ammonium) station (Fig. 18). Once **18** is protonated, the macrocycle moves away from the centre station due to weakened binding and charge repulsion. Unexpectedly, the macrocycle only stays at one phenyl triazole station that is closer to the butyl groups of the macrocycle, generating a directional shuttling. This can be explained by multiple weak interactions in $\mathbf{18H_2}^{2+}$ synergistically supporting this energy-minimized structure. The subsequent addition of NEt_3 causes rotaxane $\mathbf{18H_2}^{2+}$ to regain its original state.

3. Actuating circumrotation in catenanes

Circumrotation in catenanes is another typical mechanical motion in MIMs. In principle, all above-mentioned operating mechanisms in rotaxanes can be used in catenane architectures, giving rise to rotational motions. However, only a few examples have been successfully achieved for this goal, mainly due to the larger synthetic challenge of catenanes than rotaxanes. At the early stage, Stoddart and Sauvage[53] constructed a hybrid [2]catenane that performed circumrotation motion of one ring within the other triggered by adding acid–base. As shown in Fig. 19, the [2]catenane **19** contains a core of two dpp-type ligands (dpp = 2,9-diphenyl-1,10-phenanthroline), π-electron rich aromatic rings (1,5-dioxynaphthalene) and a π-electron deficient component (tetracationic cyclophane). Under acidic conditions, the two dpp fragments in $\mathbf{19H}^{+}$ are entwined around the proton. Under basic conditions, the **19** adopts another entwined topography for the formation of a π–π donor–acceptor complex between 1,5-dioxynaphthalene and bipyridinium.

Donor–acceptor [2]catenanes could also perform as a pH-triggered molecular switch, which was demonstrated by Stoddart. For example, [2]catenane **20** consists of a tetracationic cyclophane ($CBPQT^{4+}$) and a crown ether containing a hydroquinone(HQ) unit and a 1,5-diaminonaphthalene (DAN) unit (Fig. 20).[54] And the DAN and HQ units compete for the cavity of the $CBPQT^{4+}$ ring in a ratio of 78 : 22 in aqueous solution, giving two circumrotational isomers, **20a** and **20b**. After protonation of the DAN unit with HCl, the HQ units exclusively reside in the $CBPQT^{4+}$ ring's cavity on account of coulombic repulsion. And this switching process can be reset by adding DABCO (1,4-diazabicyclo[2.2.2]octane). This switchable rotation can be repeated more than five times by alternately adding acid and base in water. Another pH-controllable donor–acceptor [2]catenane **21** involves an extended tetracationic cyclophane ($ExBox^{4+}$) and porphyrin-containing polyether (Fig. 21).[55] The acid–base actuation depends on the protonation and deprotonation of the nitrogen atoms of the porphyrin unit. The neutral porphyrin unit resides inside the cavity of the cyclophane on account of π-associated charge-transfer interactions. Addition of TFA protonates the porphyrin ring which drives the cyclophane away from the porphyrin unit to minimize the repulsive interactions. The switch can be reversibly restored to their original structure by the addition of base. Taking advantage of the pH-responsiveness of the porphyrin

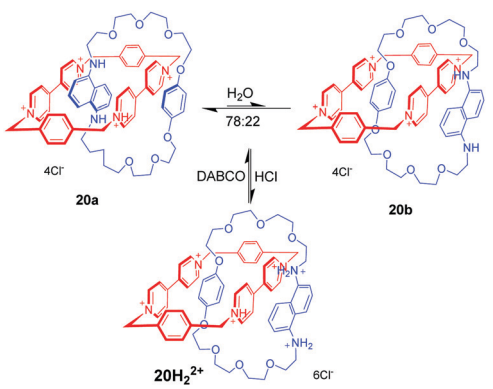

Fig. 20 A donor–acceptor [2]catenane **20** which is operated with acid–base in water.

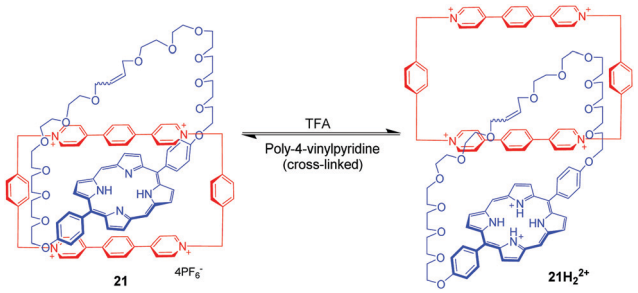

Fig. 21 pH-Controllable [2]catenane **21**.

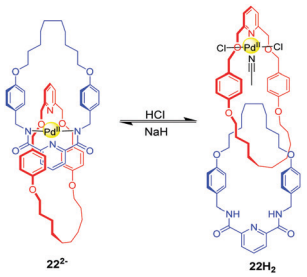

Fig. 22 Rotational motion in [2]catenane $\mathbf{22H_2}$ relies on the manipulation of palladium(II) coordination modes by acid–base.

unit, Rowan and Nolte also reported a series of acid–base switchable MIMs from porphyrin–glycoluril cage compounds.[56]

Other pH-induced circumrotational motion involves the benzylic amide macrocycle which was reported by several groups. For example, the [2]catenane $\mathbf{22H_2}$ is composed of two pyridyl rings. The mechanism of rotational motion in this catenane relies on the manipulation of palladium (II) coordination modes *via* acid–base chemistry (Fig. 22).[57] When the amide groups of the 'blue' macrocycle in $\mathbf{22H_2}$ are deprotonated with a strong base (NaH), both rings participate in the square planar coordination in $\mathbf{22}^{2-}$. After neutralization with HCl, only a 'red' ring is coordinated to the palladium metal ion, regenerating $\mathbf{22H_2}$. These different coordination modes cause a rotational motion in the catenane. Beer and co-workers also reported a pH-switchable [2]catenane **23H** driven by anion recognition.[58] This catenane comprises a pyridinium-based isophthalamide ring and a phenolic containing ring (Fig. 23). Initially, two rings intertwine in **23H** with the pyridinium ring motif between the electron rich hydroquinone groups stabilized by aromatic donor–acceptor interactions and hydrogen bonds. Upon the addition of base, the phenol group is deprotonated to form a phenolate anion, and the rings undergo a circumrotation so that the phenolate anion can associate with pyridinium bis-amide *via* hydrogen bonding. The rotation process can be reversed with the addition of TFA. Lin and co-workers reported the pyridyl amide [2]catenane containing two pyridyl macrocycles and one of them was modified with tetraphenylethene (TPE).[59] The acid–base controllable rotation endows it with enabled aggregation-induced emission.

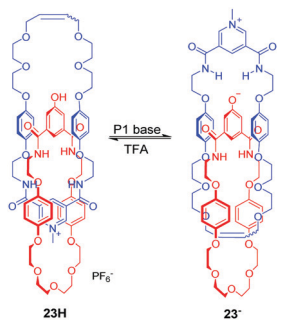

Fig. 23 pH-Switchable [2]catenane **23H** driven by anion recognition.

4. pH-Controlled motions beyond translocation and circumrotation

To date, most of the design motifs involved in synthesized molecular machines are based on relatively simple MIMs that execute a single movement of subcomponents. Actually, the artificial molecular machines are expected to perform more sophisticated tasks like natural machines. Although it is impossible to attain by the current generation of molecular machines, scientists have been trying to explore some of the advances by applying the basic principles in rotaxanes and catenanes.[60] Several specific topological architectures constricted by mechanical bonds are adopted to carry out the sophisticated tasks inspired by nature. Representative examples include molecular elevators,[61] molecular muscles,[62] molecular ratchets[63] and so on. pH-Stimulation is proved to be the most efficient means to fulfil this challenge. In this section, we will present how to operate several sophisticated motions in MIMs by acid–base chemistry.

4.1 Molecular elevators

The advent of molecular elevators is a landmark of synthesized molecular machines, which was firstly reported by Stoddart's group in 2004.[61] Molecular elevators are a class of rotaxanes which express the up-and-down motion of their platform component interlocked with a rig-like component. As shown in Fig. 24, the triply interlocked rotaxane $\mathbf{24H_3}^{3+}$ is made up of a multivalent platform of rings containing three crown ether macrocycles and the trifurcated rig-like component possesses dibenzylammonium and $BIPY^{2+}$ recognition sites. The movement of the elevator

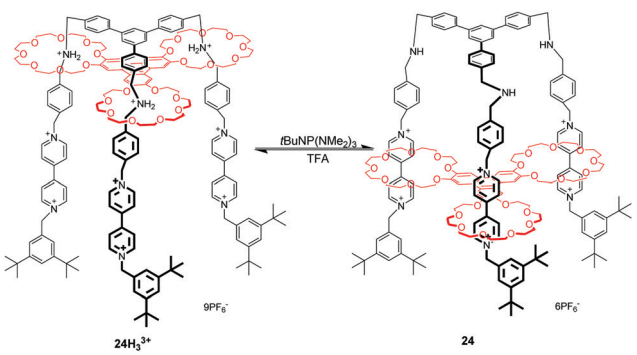

Fig. 24 Stoddart's molecular elevator.

depends on the protonation and deprotonation of the dibenzylammonium ions with acid and base. It has been estimated from a thermodynamic analysis that the elevator movement from the upper to lower level could generate a force of up to 200 pN. When investigating how the rig and platform components move with respect to each other, they found that the translational motions of each ring operate in a stepwise manner, rather than by a concerted motion of the entire platform, owing to the conformational flexibility of the rig.[64] This well-defined mechanical movement also reveal that the multivalent compounds can be harnessed to perform nontrivial mechanical movements.[65]

Another example of a molecular elevator was introduced by Tanaka[66] in the form of four-fold rotaxane $\mathbf{25H_4}^{4+}$, in which the Cu(II) porphyrin rig with four alkylammonium chains is mechanically linked to crown ethers of a Cu(II) phthalocyanine tetramacrocycle by a facial stacking (Fig. 25). The spin–spin interactions between the Cu^{2+} centers are sensitively influenced by their distance and relative spatial configuration. This expectation was confirmed by electron paramagnetic resonance (EPR) spectroscopy, which revealed that the spin-exchange interactions occur only in compressed **25** and not in $\mathbf{25H_4}^{4+}$. By acid–base stimuli, the switchable spin–spin communication between mechanically interlocked metal complexes was well demonstrated. This concept would encourage us to prepare the supramolecular architectures with switchable functions related to nanomagnetism, conductivity, and photonic properties.

pH-Controlled palindromic motions also have been exploited to tune the interaction between naphthalene diimide (NDI) and anthracene chromophores in a double-leg donor–acceptor molecular elevator $\mathbf{26H_2}^{2+}$.[67] As shown in Fig. 26, a bis-24C8 macrocycle with an electron-rich anthracene moiety in the middle was chosen for the platform component, and the rig component contains a NDI unit with dialkylammonium and methyl triazolium

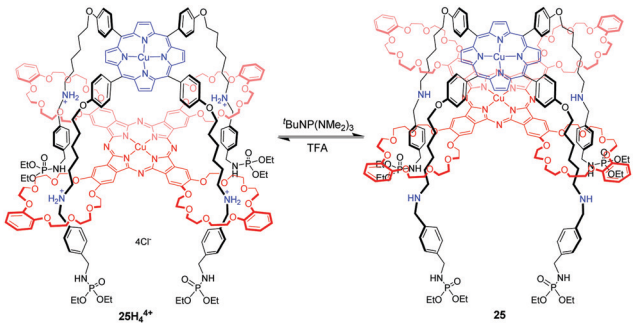

Fig. 25 Tanaka's molecular elevator.

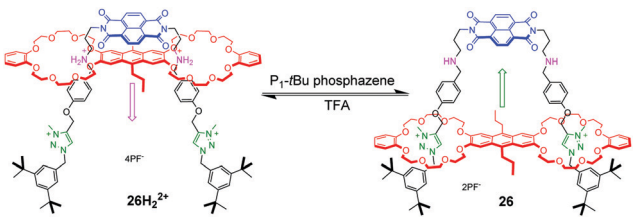

Fig. 26 Double-leg donor–acceptor molecular elevator **26**.

stations on its legs. The distance between the two different platforms can be adjusted by acid and base. The similar operation of a bipodal molecular elevator with a ferrocene platform was also demonstrated by Qu.[68]

4.2 Contracting and stretching motion in [c2]daisy chains

Molecular muscles, which exhibit expansion and contraction on the nanoscale, are another typical mode of motion by mimicking biology. Rotaxane architectures, especially supramolecular daisy chains,[69] have been a promising candidate for the design and synthesize of artificial molecular muscles.[70] A daisy chain is a special case of MIMs created by interlocked monomers that consist of both a linear thread (guest) and a ring (host). In these systems, shuttling of the macrocycle along the thread results in a relative motion that either contracts or expands the entire molecule under the external stimuli.

[c2]Daisy chains, with double-threaded architecture of the rotaxane dimer, are an ideal module for the construction of artificial molecular muscles by means of antiparallel sliding among its two interlocked rings. A large proportion of [c2]daisy chains are based on crown ethers and dialkylammonium ions, where contracting and stretching motions are readily actuated by acid/base. Stoddart and co-workers[71] for the first time reported the pH-controllable [c2]daisy chain, in which the two DB24C8 rings switch between two different recognition sites, dibenzylammonium and bipyridinium. As a result, the $\mathbf{27H_2}^{2+}$ adopted an extended state under acidic conditions, or a contracted state in **27** under basic conditions, in a similar manner to human muscles (Fig. 27). The simulation results show that the longitudinal molecular length of deprotonated **27** became approximately 29% (0.9 nm) shorter than the original extended length in $\mathbf{27H_2}^{2+}$. Analogous to this operating mechanism, Coutrot and co-workers[72] prepared the pH-switchable [c2]daisy chain $\mathbf{28H_2}^{2+}$ by substitution of bipyridinium units with their triazolium units (Fig. 28).

In order to amplify the molecular level movements into nanoscale or microscale motions, these [c2]daisy chain topologies have been incorporated into polymer scaffolds so as to generate mechanically interlocked macromolecules. Stoddart and co-workers[73] synthesized a bistable poly[c2]daisy chain $\mathbf{29H_n}^{n+}$ using click chemistry (Fig. 29). This mechanically interlocked polymer had **11** repeating [c2]daisy chain monomers on average.

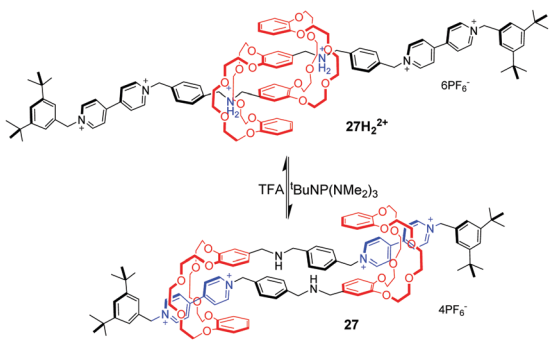

Fig. 27 pH-Actuated [c2]daisy chain **27**.

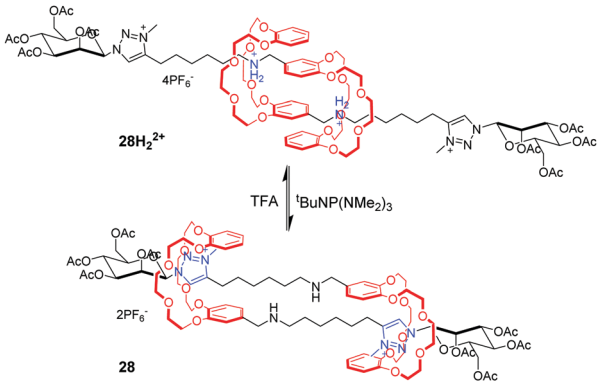

Fig. 28 Coutrot's type of [c2]daisy chain.

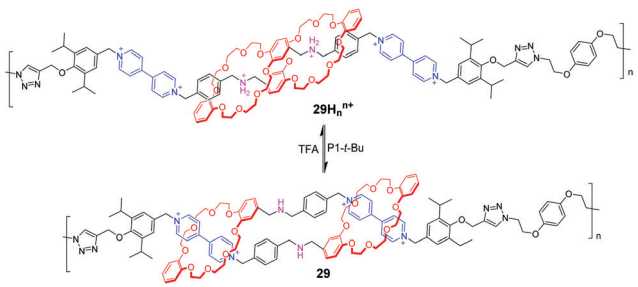

Fig. 29 Acid–base actuation of [c2]daisy chains **29**.

The experiments confirmed that a concerted contractile motion is indeed achievable along a polymer backbone by acid and base. They also found that the extension/contraction movements of the polymeric [c2]daisy chain are actually faster than those of the corresponding monomer. These observations demonstrate important information that the complexity of MIMs will promote their performance in materials.

By utilizing olefin metathesis, Grubbs and co-workers[74] synthesized a [c2]daisy chain dimer with the ammonium binding site. With addition of potassium hydroxide, the ammonium is deprotonated to give the unbound analogue due to the absence of a secondary binding site. Then, the system can be reset to the contracted, bound conformation by hexafluorophosphoric acid, enhancing its utility as a synthetic molecular actuator. Subsequently, the click polymerization of this [c2]daisy chain gives a linear polymer $\mathbf{30H}_n^{n+}$, which possesses about **22** repeating units. Like the monomeric dimer, the polymer could also be readily deprotonated and reprotonated by alternately adding base and acid (Fig. 30). The multiangle laser light scattering (MALLS) detection analysis showed that the polymer had a radius of gyration (R_g) of 14.8 nm in the contracted conformation. Deprotonation of $\mathbf{30H}_n^{n+}$ to generate **30** did not induce lengthening (R_g = 13.5 nm), likely due to poor solubility and π–π slipped-stacking interactions, but acylated polymer **30a** showed a 48% increase in size (R_g = 21.4 nm).

In the cases of Stoddart and Grubbs, the low molecular weight problem impeded the performance of the poly[c2]daisy chain in actuating contractile motions on mesoscopic scales. Giuseppone *et al.*[75] solved this problem by taking metallosupramolecular polymerization of the [c2]daisy chain monomers.

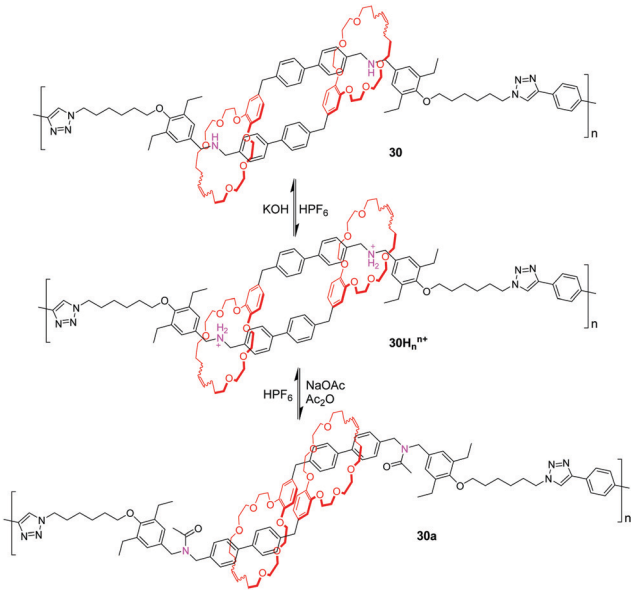

Fig. 30 pH-Controllable [c2]daisy chain dimer polymer.

They synthesized a [c2]daisy chain analogous to Coutrot's **28**, which featured terpyridines as stoppers. The addition of Zn(II) or Fe(II) triggered the supramolecular polymerizations of the [c2]daisy chain dimer for the formation of the bisterpyridine complexes. As a result, more than 3000 repeating units were embedded into a single-strand polymer chain. Thus, the poly[c2]daisy chains can amplify the tiny motions of rotaxane-based molecular muscles by four orders of magnitude. The X-ray scattering experiments revealed that the contour length of the protonated polymer $\mathbf{31H}_n^{n+}$ (Fig. 31) is longer (15.9 μm) compared to the deprotonated polymer (9.4 μm). The same group also demonstrated that [c2]daisy chains of this type can be modified with alternative stoppering groups to induce the fabrication of other supramolecular polymers, and that the pH-actuated contractile motions influence the morphologies of the corresponding aggregates.[76]

4.3 Tightening and loosening in lasso rotaxanes

[c1]Daisy chains, also known as lasso, are the simplest rotaxanes in the family of daisy chains. Due to their unique self-entangled structure, the tightening and loosening motions can be achieved

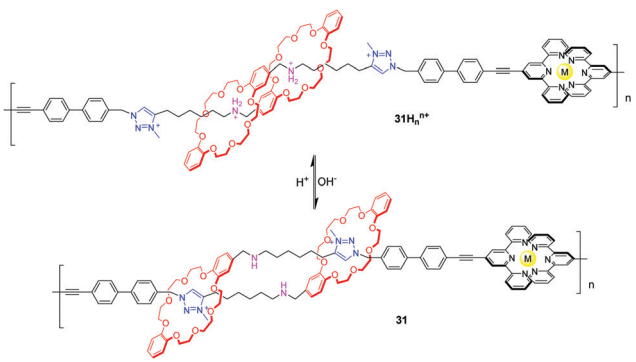

Fig. 31 pH-Controllable metallosupramolecular poly[c2]daisy chain.

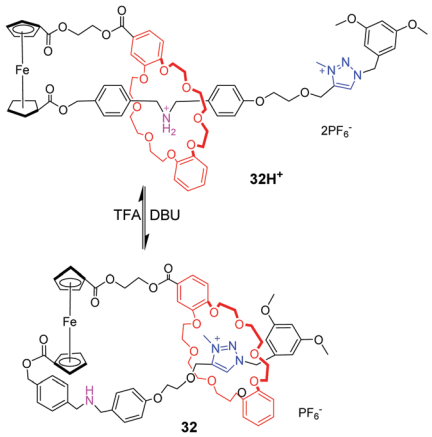

Fig. 32 pH-Switchable lasso rotaxane **32**.

by gliding of the ring between different stations. Several examples of pH-responsive [c1] daisy chains are based on dialkylammonium and crown ether recognition motifs. An early example was reported by Qu and co-workers,[77] in which a ferrocene unit as an electrochemically active centre is covalently linked to the DB24C8 macrocycle and a thread with a dibenzylammonium site (DBA) and a *N*-methyltriazolium (MTA) site (Fig. 32). In the protonated state, the DB24C8 encircles the DBA station in **32H**$^+$, which makes the ferrocene unit show a reversible oxidation–reduction property. Upon deprotonating the ammonium with base, the DB24C8 moves to the MTA site in **32**, resulting in the electrochemically irreversible state. This switchable motion was also designed for application in fluorescence output.[78] As shown in Fig. 33, the [1]rotaxane **33H**$^+$ comprises a ferrocenyl (Fc) unit covalently connected with a DB24C8 macrocycle and a thread with different stations. The 4-morpholinnaphthalimide (MA) was chosen as a terminated stopper, whose fluorescence could be adjusted on and off by a distance-dependent photo-induced electron transfer (PET) process between an electron-rich Fc unit and an electron-deficient MA fluorophore. Under acidic conditions, the DB24C8 resides in the ammonium site forcing the lasso to adopt a tightened co-conformation. At this point, the ferrocenyl unit remains too far away from the morpholin–naphthalimide to quench its fluorescence, the latter being monitored by the naked eye. Deprotonation of the ammonium results in the shuttling of the DB24C8 around the triazolium, hence loosening the lasso. In this specific co-conformation, the ferrocenyl unit is much closer to the tail, now authorizing a strong PET from the electron-rich ferrocene to the electron-deficient naphthalimide. Furthermore, the fluorescence output signal was also redox-dependent by oxidizing/reducing the ferrocene unit.

Qu *et al.* has also investigated the pH-controlled molecular motions of a multifunctional bis-branched [1]rotaxane with reversible fluorescence changes and tunable molecular aggregations.[79] As shown in Fig. 34, bis[1]rotaxane **34H$_2$**$^{2+}$ comprises a perylene-bisimide (PBI) core and two bistable [1]rotaxane arms containing two different stations and terminal ferrocene units. The translational movement of the DB24C8 between ammonium and triazolium units can be controlled by acid/base, giving rise to a change in molecular length of about 1.7 nm. Interestingly, the molecular dynamics simulations indicated that these extension and contraction movements were accompanied by a simultaneous rotational motion of the ferrocene units, thus generating a dual-mode movement type. More importantly, the movement of DB24C8 rings can adjust the system fluorescence through the PET process and nano-structural morphologies induced by PBI aggregations with Zn^{2+}. The same group later adapted this ferrocene-linked [1]rotaxane into a more complex star-shaped [1](n)rotaxane, including tris[1]rotaxane and tetrakis[1]rotaxane, which expand and contract radially in response to pH changes.[80]

Coutrot *et al.* also have stimulated remarkable progress toward pH-controlled motions in lasso rotaxanes.[81] They ingeniously described the constriction and dilation of a double-lasso architecture (Fig. 35), which derives from an end-activated [c2]daisy chain. The two DB24C8 rings can slide along the ultramacrocyclic loop upon variation of pH. At low pH, the double lasso adopts a

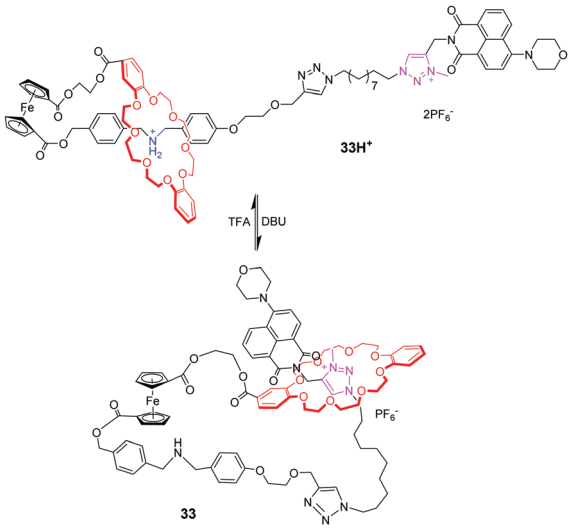

Fig. 33 Lasso rotaxane **33** with switchable fluorescence output.

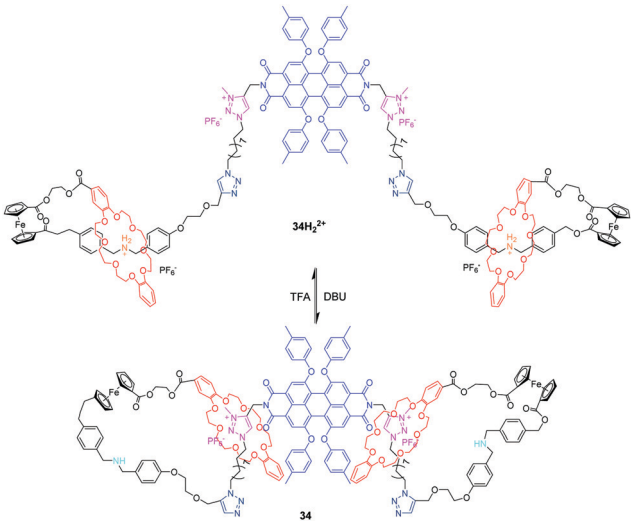

Fig. 34 pH-Controllable bis[1]rotaxane **34**.

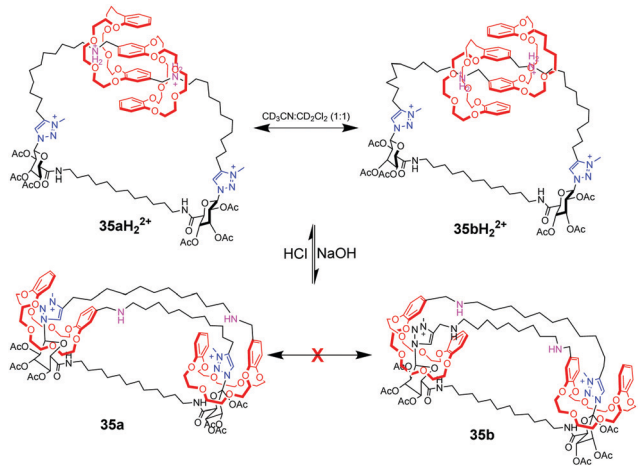

Fig. 35 pH-Triggered motion in double-lasso architecture.

relatively loose conformation, allowing fast exchange between isomers $\mathbf{35aH_2}^{2+}$ and $\mathbf{35bH_2}^{2+}$, thus behaving like a "jump rope". The addition of base triggered the shuttling motion of the DB24C8 around the triazolium stations, generating a tightened conformation. In this conformation, the jump rope movement was inhibited.

4.4 Wing-flapping motion in a [2](2)rotaxane

By imitating bionic machines, Chen and co-workers[82] constructed a novel [2](2)rotaxane based on a pentiptycene-derived bis(crown ether) host. It was found that the shuttle process of two DB24C8 rings between the dibenzylammonium and *N*-methyltriazolium stations can be operated by acid/base stimulus. In the protonated state, two DB24C8 encircle the ammonium station without any torsion of the host. Deprotonation of the ammonium ion with DBU causes the movement of DB24C8 to triazolium stations, just like a butterfly spreading its wings (Fig. 36).

4.5 Molecular pulley

Chen *et al.* reported a pulley-like motion of the triply interlocked [2]rotaxane, which combines the features of plain rotary motion and linear translocation.[83] In $\mathbf{37H_3}^{3+}$ as shown in Fig. 37, the triptycene-derived tris(crown ether) host (TC), with three DB24C8 rings positioned in three orientations, threads onto a

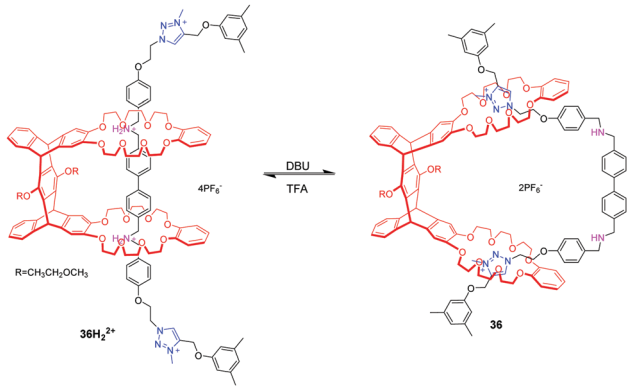

Fig. 36 pH-Driven wing-flapping motion in a [2](2)rotaxane **36**.

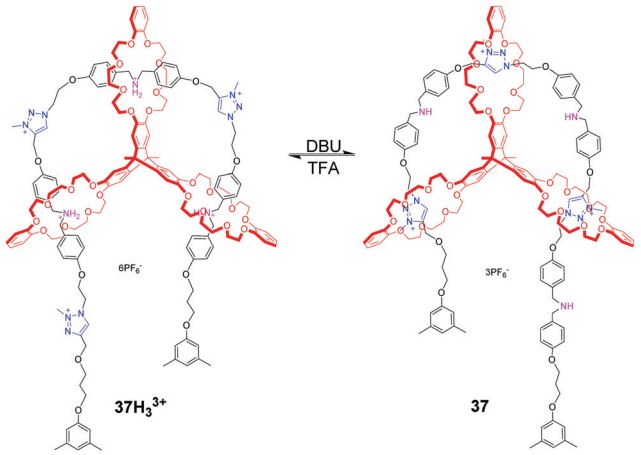

Fig. 37 pH-Controlled molecular pulley based on a triply interlocked [2]rotaxane **37**.

linear molecular axle which incorporates three dibenzylammonium and three *N*-methyltriazolium sites. And the three DB24C8 rings all encircle ammonium salt sites. Upon deprotonating these sites with DBU, each DB24C8 shuttles to the triazolium station, generating the direction-biased motion. The sliding back of the dibenzylammonium sites into the DB24C8 rings is possible through reprotonation of the amines using TFA. As a result, the back and forth motion in an arc-shaped trajectory was found in this [2]rotaxane, mimicking the function of the fundamental pulley device. This work presents a new mode of motion that combines translocation and circumrotation in a typical [2]rotaxane and [2]catenane.

4.6 Stepwise motion in a multivalent [2](3)catenane

Based on a pyrazine-extended triptycene-derived tris-(crown ether) host (eTC), another unique topologically linked interlocked molecule, [2](3)catenane $\mathbf{38H_3}^{3+}$ (Fig. 38), was also reported by

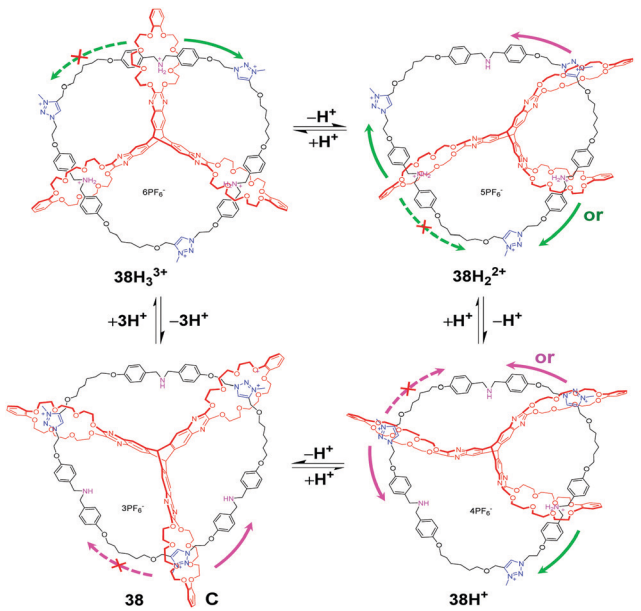

Fig. 38 Stepwise motion in [2](3)catenane 38 actuated by acid–base.

Chen's group.[84] The three crown ether of eTC successively threads onto a circular ditopic guest with three dibenzyl ammonium (DBA) sites and three *N*-methyltriazolium (MTA) sites. Taking advantage of the multivalent nature featuring multiple and sequential binding, the acid–base triggered motion can be actuated in a stepwise manner. As the DBU is added to deprotonate the DBA sites, one of three crown ether rings in $\mathbf{38H_3}^{3+}$ begins to move to the MTA site, then two, and finally all three rings encircle the MTA sites. Thus, the four protonation states of the [2](3)catenane can be detected and identified by ^{1}H NMR titration experiments, which confirms the multistep process. And the different thermodynamic data of dissociation equilibria, corresponding to pK_a values was also determined by an indicator method. Moreover, an uncontemplated selectivity in the stepwise motion was observed where the B24C8 ring exclusively moved to nearer the MTA sites in $\mathbf{38H_3}^{3+}$ owing to the special interlocked topology of the [2](3)catenane.

5. Controlling pH-responsive motions by alternative stimuli

Although acids and bases have been an efficient and commonly used stimuli for pH-responsive motions, the energy supply strategy is relatively simple. Besides, the waste products generated from acid–base neutralization reaction accumulate and will eventually affect the operation of the systems. Hence, the utilization of alternative stimuli instead of acids and bases will improve the performance of molecular machines. In this regard, a decarboxylation of strategy was used to power acid–base operated molecular machines. Photo-induced proton-transfer strategy was incorporated into pH-responsive molecular switches. Recently, a step-by-step reaction with pH oscillating properties has been found to power translational motion triggered by a chemical fuel pulse. In the following section, we will give a detailed introduction about this progress.

Taking advantage of pH-responsiveness of ammonium/crown ether-type MIMs, Takata and co-workers[85] constructed a thermo-responsive rotaxane shuttling system. As shown in Fig. 39, the [2]rotaxane $\mathbf{39H}^+$ is equipped with a trichloroacetate counterion (CCl_3COO^-), which is the key feature. Under the condition of heat, the CCl_3COO^- extracts a proton from the dibenzylammonium group and undergoes thermal decomposition to CO_2 gas and volatile $CHCl_3$. In the meantime, the macrocycle moves away from the nitrogen atom to generate the neutral rotaxane **39**. The $\mathbf{39H}^+$ is reproduced by the addition of trichloroacetic acid (CCl_3COOH), providing a novel switching system. More importantly, this shuttling motion was well-repeated without accumulated residues of the salts compared to previous acid–base stimuli. Later, they embedded this thermoresponsive rotaxane in the side chains of poly[2]rotaxanes to control the helical pitch of a polyacetylene backbone.[86]

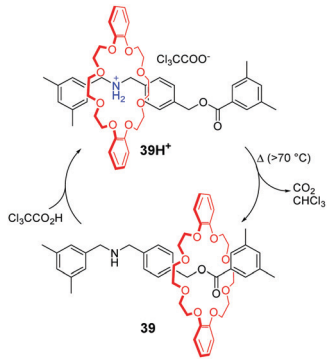

Fig. 39 Decarboxylation of trichloroacetate counteranions driving the shuttling motion.

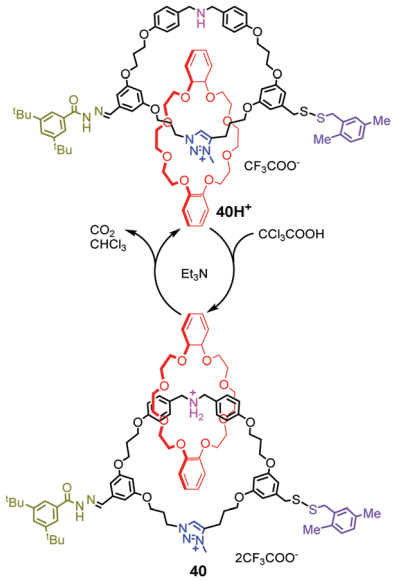

Fig. 40 Operation of a rotary motor using base-promoted decarboxylation.

A similar decarboxylation strategy was also introduced into rotary and linear molecular motors by Leigh's group[87] They designed an energy ratchet mechanism based on acid–base oscillations that power molecular motors. The acid–base oscillations are operated by base-promoted decarboxylation of CCl_3COOH. As shown in Fig. 40, [2]catenane $\mathbf{40H}^+$ comprises two interlocked rings: a crown ether ring and a larger ring with a dibenzylamine unit, triazolium site and two potential blocking groups. Upon addition of excess CCl_3COOH, the dibenzylamine site is protonated and the hydrazone undergoes exchange *via* a transient aldehyde, leading to 180° directional rotation. In the meantime, triethylamine catalyzes decarboxylation of the trichloroacetic acid, generating CO_2 and $CHCl_3$. And the reaction solution becomes sufficiently basic to deprotonate the dibenzylammonium group and promote disulfide exchange, which resulted to another 180° directional rotation of the motor. As a whole, the crown ether completes one 360° directional rotation after one acid–base cycle. Based on this operating mechanism, [3]catenane rotary molecular motors and a linear molecular pump were also realized. Recently, they reported that a rotaxane catalyst can be switched using CCl_3COOH as fuel pulses.[88]

2-Cyano-2-phenylpropanoic acid is another choice of substrate for acid–base responsive molecular switching by the strategy of

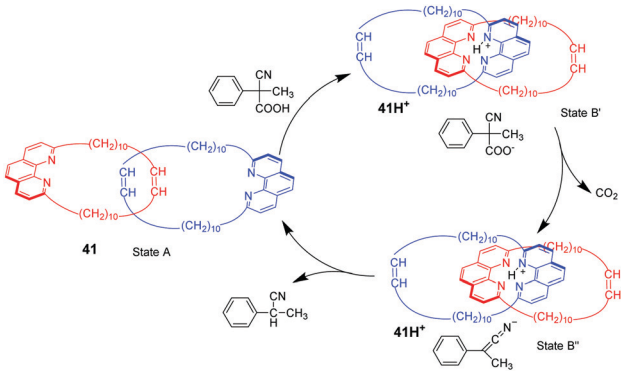

Fig. 41 Switching motions of catenane **41** fueled by 2-cyano-2-phenylpropanoic acid.

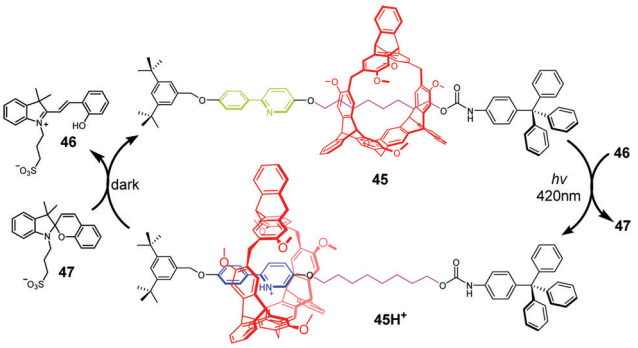

Fig. 43 Reversible shuttling motion controlled by photoacid.

decarboxylation reaction, which has been reported by Stefano and co-workers.[89] As shown in Fig. 41, [2]catenane **41** consists of two identical interlocked macrocycles featuring 1,10-phenanthroline units in their backbone without any precisely defined co-conformation (state A). The addition of 2-cyano-2-phenylpropanoic acid can provide protons to stabilize the ternary complex (state B′) by hydrogen bonding, producing the proton catenate **41H**$^+$. Then, 2-cyano-2-phenylpropanoic acid can undergo smooth decarboxylation in the presence of NEt_3, leading to state B″. Finally, rate-determining proton transfer from **41H**$^+$ to the anion, restores the catenane to its neutral form **41**. This process demonstrated an autonomous back and forth motion by tactful coupling of the decarboxylation of 2-cyano-2-phenylpropanoic acid to an acid–base operated [2]catenane. Later, Schmittel and co-workers employed 2-cyano-2-phenylpropanoic acid as a chemical fuel to switch a [2]rotaxane shuttle with a feature of oscillating emission.[90]

Photoacids or photobases, which exhibit an increase in their acidity or basicity upon photoexcitation, provide a new method to drive acid–base switchable molecular machines through a photo-induced proton-transfer (PIPT) strategy. Jiang and co-workers[91] firstly reported a non-photoresponsive molecular shuttle coupled to a photoacid. In the [2]rotaxane **42** (Fig. 42), the DB24C8 resides at the triazolium station. The photoacid **43** can protonate the dibenzylamine after irradiation by a 365 nm ultraviolet lamp, generating **42H**$^+$. However, they failed to trigger the deprotonation step in the dark to reset the system to its original state. In order to find a more compatible system, Chen and coworkers developed an acid/base responsive complexation between helic[6]arene and pyridinium, which can be efficiently controlled by coupling to a photoacid.[92] Subsequently, they designed and synthesized the [2]rotaxane **45** featuring the helic[6]arene/pyridinium recognition motif. It was found that photoacid **46** could protonate the pyridine part of **45** after 420 nm light or sunlight irradiation, which induces the macrocycle to move to the pyridium site from the alkyl group site. Moreover, the systems can be reversibly restored to their original structures under dark conditions. This acid/base-controlled palindromic motion could be switched repeatedly more than 50 times with excellent reproducibility (Fig. 43).

Recently, Chen *et al.* reported a new step-by-step reaction system with a pH oscillation feature that powers the acid–base controllable molecular shuttle.[93] The rotaxane **48H**$^+$ (Fig. 44) is composed of a helic[6]arene interlocked onto a thread, which has a protonated pyridinium site and the alkyl chain site. The pH oscillation reaction-powered motion of the rotaxane was triggered by PhIO, which was considered as a fuel input. The PhIO can absorb the TFA from **48H**$^+$ to produce [bis(trifluoroacetoxy)iodo]benzene (BTAIB), leading to the movement of the macrocycle to the alkyl group in **48**. Then, the newly produced BTAIB could be utilized to participate in the TEMPO-catalyzed oxidation of isopropanol to acetone. In the meantime, TFA could be gradually released from BTAIB,

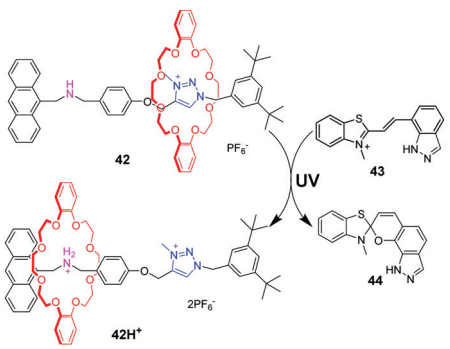

Fig. 42 Light-controlled switching of the pH-responsive molecular shuttle.

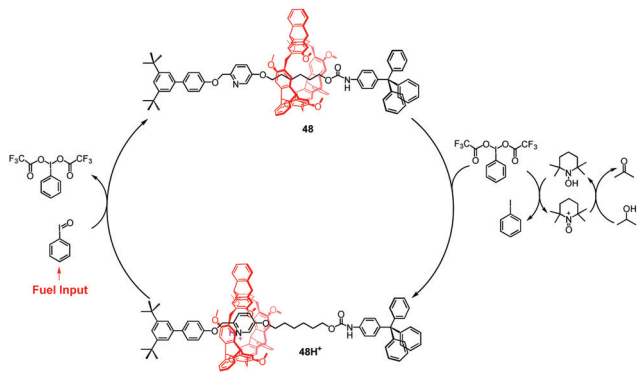

Fig. 44 Switchable motion of the [2]rotaxane powered by step-by-step reaction.

which resulted in the formation of **48H**$^+$ again. This work represents the new pH oscillating chemical fuel powered mechanical movement of a molecular shuttle.

6. Summary and outlook

In this review, we summarized the pH-controlled motions that arise as a result of a mechanical bond. These motions involve non-covalent interactions, including hydrogen bonding, hydrophobic effects, electrostatic interactions and others, and are usually sensitive to pH variation, which makes them one of the most powerful and commonly used means of controlling molecular motions. By adopting different host–guest recognition motifs, two types of motions including translocations in rotaxanes and circumrotations in catenanes could be efficiently controlled by acid–base chemistry. By integrating these simple movements, more diverse and sophisticated motions at the molecular level have been realized as well. These highly complex molecular machines would stimulate remarkable improvement toward understanding physics and biology. Finally, we also highlighted the pH-dependent motions controlled by alternative stimuli instead of acids and bases, which could overcome the disadvantages of acid–base stimuli and generate novel modes of motion.

We believe that pH-stimulation will continue to play a key role in artificial molecular machines, particularly in multivalent and multicomponent systems. By integrating the operating mechanisms that appeared in this review, we might realize more complex molecular-level motion like biological molecular machines. Moreover, the introduction of various functional groups into MIMs is also helpful to construct pH-responsive functional materials.[94] Last but not least, pH gradients are widespread in biological and physiological systems, which can provide the perfect environment for us to power molecular motions in living organisms. Taking advantage of pH gradients, we might operate molecular shuttles in lipid bilayers for transmembrane transport,[95] and adopt [2]rotaxane as a nanovalve to selectively modulate drug release.[96] We can foresee that this combination might promote the application of artificial molecular machines in biology and medicine.

Conflicts of interest

There are no conflicts to declare.

Acknowledgements

We thank the National Natural Science Foundation of China (21772205, 21521002) for financial support.

Notes and references

1 (*a*) J. F. Stoddart, *Chem. Soc. Rev.*, 2009, **38**, 1802; (*b*) L. Fang, M. A. Olson, D. Benítez, E. Tkatchouk, W. A. Goddard Iii and J. F. Stoddart, *Chem. Soc. Rev.*, 2010, **39**, 17.
2 S. D. P. Fielden, D. A. Leigh and S. L. Woltering, *Angew. Chem., Int. Ed.*, 2017, **56**, 11166.
3 C. J. Bruns and J. F. Stoddart, *The Nature of the Mechanical Bond: From Molecules to Machines*, Wiley, 2016.
4 (*a*) V. Balzani, A. Credi, F. M. Raymo and J. F. Stoddart, *Angew. Chem., Int. Ed.*, 2000, **39**, 3348; (*b*) J. F. Stoddart, *Angew. Chem., Int. Ed.*, 2014, **53**, 11102; (*c*) S. Erbas-Cakmak, D. A. Leigh, C. T. McTernan and A. L. Nussbaumer, *Chem. Rev.*, 2015, **115**, 10081.
5 (*a*) J. F. Stoddart, *Angew. Chem., Int. Ed.*, 2017, **56**, 11094; (*b*) J.-P. Sauvage, *Angew. Chem., Int. Ed.*, 2017, **56**, 11080; (*c*) B. L. Feringa, *Angew. Chem., Int. Ed.*, 2017, **56**, 11060.
6 M. Xue, Y. Yang, X. Chi, X. Yan and F. Huang, *Chem. Rev.*, 2015, **115**, 7398.
7 G. Gil-Ramírez, D. A. Leigh and A. J. Stephens, *Angew. Chem., Int. Ed.*, 2015, **54**, 6110.
8 (*a*) C. J. Bruns and J. F. Stoddart, *Acc. Chem. Res.*, 2014, **47**, 2186; (*b*) S. Kassem, T. van Leeuwen, A. S. Lubbe, M. R. Wilson, B. L. Feringa and D. A. Leigh, *Chem. Soc. Rev.*, 2017, **46**, 2592.
9 (*a*) A. Carlone, S. M. Goldup, N. Lebrasseur, D. A. Leigh and A. Wilson, *J. Am. Chem. Soc.*, 2012, **134**, 8321; (*b*) Z. Meng, J.-F. Xiang and C.-F. Chen, *Chem. Sci.*, 2014, **5**, 1520; (*c*) M. R. Wilson, J. Solà, A. Carlone, S. M. Goldup, N. Lebrasseur and D. A. Leigh, *Nature*, 2016, **534**, 235.
10 (*a*) M. Baroncini, S. Silvi, M. Venturi and A. Credi, *Angew. Chem., Int. Ed.*, 2012, **51**, 4223; (*b*) G. Ragazzon, M. Baroncini, S. Silvi, M. Venturi and A. Credi, *Nat. Nanotechnol.*, 2015, **10**, 70; (*c*) M. Baroncini, M. Canton, L. Casimiro, S. Corra, J. Groppi, M. La Rosa, S. Silvi and A. Credi, *Eur. J. Inorg. Chem.*, 2018, 4589; (*d*) D.-H. Qu, Q.-C. Wang, Q.-W. Zhang, X. Ma and H. Tian, *Chem. Rev.*, 2015, **115**, 7543.
11 (*a*) C. Pezzato, M. T. Nguyen, D. J. Kim, O. Anamimoghadam, L. Mosca and J. F. Stoddart, *Angew. Chem., Int. Ed.*, 2018, **57**, 9325; (*b*) Y. Wang, T. Cheng, J. Sun, Z. Liu, M. Frasconi, W. A. Goddard and J. F. Stoddart, *J. Am. Chem. Soc.*, 2018, **140**, 13827; (*c*) H. V. Schröder, F. Stein, J. M. Wollschläger, S. Sobottka, M. Gaedke, B. Sarkar and C. A. Schalley, *Angew. Chem., Int. Ed.*, 2019, **58**, 3496.
12 (*a*) K. C.-F. Leung, C.-P. Chak, C.-M. Lo, W.-Y. Wong, S. Xuan and C. H. K. Cheng, *Chem. – Asian J.*, 2009, **4**, 364; (*b*) G.-H. Weng, B. Zhu, Y. Ye and S. Li, *Chin. J. Org. Chem.*, 2015, **35**, 309.
13 (*a*) J. W. Lee, S. Samal, N. Selvapalam, H.-J. Kim and K. Kim, *Acc. Chem. Res.*, 2003, **36**, 621; (*b*) L. Isaacs, *Acc. Chem. Res.*, 2014, **47**, 2052.
14 W. L. Mock and J. Pierpont, *J. Chem. Soc., Chem. Commun.*, 1990, 1509.
15 S. Im Jun, J. W. Lee, S. Sakamoto, K. Yamaguchi and K. Kim, *Tetrahedron Lett.*, 2000, **41**, 471.
16 J. W. Lee, K. Kim and K. Kim, *Chem. Commun.*, 2001, 1042.
17 (*a*) D. Tuncel, Ö. Özsar, H. B. Tiftik and B. Salih, *Chem. Commun.*, 2007, 1369; (*b*) D. Tuncel and M. Katterle, *Chem. – Eur. J.*, 2008, **14**, 4110.
18 D. Tuncel, N. Cindir and Ü. Koldemir, *J. Incl. Phenom. Macrocycl. Chem.*, 2006, **55**, 373.
19 (*a*) V. Sindelar, S. Silvi and A. E. Kaifer, *Chem. Commun.*, 2006, 2185; (*b*) W. Wu, S. Song, X. Cui, T. Sun, J.-X. Zhang and X.-L. Ni, *Chin. Chem. Lett.*, 2018, **29**, 95.

20 E. J. Dale, N. A. Vermeulen, M. Juríček, J. C. Barnes, R. M. Young, M. R. Wasielewski and J. F. Stoddart, *Acc. Chem. Res.*, 2016, **49**, 262.
21 B. Odell, M. V. Reddington, A. M. Slawin, N. Spencer, J. F. Stoddart and D. J. Williams, *Angew. Chem., Int. Ed. Engl.*, 1988, **27**, 1547–1550.
22 R. A. Bissell, E. Córdova, A. E. Kaifer and J. F. Stoddart, *Nature*, 1994, **369**, 133.
23 M. Martínez-Díaz, N. Spencer and J. F. Stoddart, *Angew. Chem., Int. Ed. Engl.*, 1997, **36**, 1904.
24 P. R. Ashton, R. Ballardini, V. Balzani, I. Baxter, A. Credi, M. C. Fyfe, M. T. Gandolfi, M. Gómez-López, M. Martínez-Díaz and A. Piersanti, *J. Am. Chem. Soc.*, 1998, **120**, 11932.
25 S. Garaudée, S. Silvi, M. Venturi, A. Credi, A. H. Flood and J. F. Stoddart, *ChemPhysChem*, 2005, **6**, 2145.
26 X. Ma, J. Zhang, J. Cao, X. Yao, T. Cao, Y. Gong, C. Zhao and H. Tian, *Chem. Sci.*, 2016, **7**, 4582.
27 F. Coutrot and E. Busseron, *Chem. – Eur. J.*, 2008, **14**, 4784.
28 (*a*) F. Coutrot, *ChemistryOpen*, 2015, **4**, 556; (*b*) P. Waelès, K. Fournel-Marotte and F. Coutrot, *Chem. – Eur. J.*, 2017, **23**, 11529; (*c*) S. Chao, C. Romuald, K. Fournel-Marotte, C. Clavel and F. Coutrot, *Angew. Chem., Int. Ed.*, 2014, **53**, 6914; (*d*) M. Berg, S. Nozinovic, M. Engeser and A. Lützen, *Eur. J. Org. Chem.*, 2015, 5966; (*e*) G. Ragazzon, A. Credi and B. Colasson, *Chem. – Eur. J.*, 2017, **23**, 2149; (*f*) Z. Meng, J.-F. Xiang and C.-F. Chen, *J. Am. Chem. Soc.*, 2016, **138**, 5652.
29 (*a*) R. Arumugaperumal, V. Srinivasadesikan, M. V. Ramakrishnam Raju, M.-C. Lin, T. Shukla, R. Singh and H.-C. Lin, *ACS Appl. Mater. Interfaces*, 2015, **7**, 26491; (*b*) W. Zhou, H. Zhang, H. Li, Y. Zhang, Q.-C. Wang and D.-H. Qu, *Tetrahedron*, 2013, **69**, 5319; (*c*) W. Yang, Y. Li, J. Zhang, Y. Yu, T. Liu, H. Liu and Y. Li, *Org. Biomol. Chem.*, 2011, **9**, 6022.
30 Q. Jiang, H.-Y. Zhang, M. Han, Z.-J. Ding and Y. Liu, *Org. Lett.*, 2010, **12**, 1728.
31 W. Yang, Y. Li, J. Zhang, N. Chen, S. Chen, H. Liu and Y. Li, *Small*, 2012, **8**, 2602.
32 (*a*) Z.-Q. Cao, H. Li, J. Yao, L. Zou, D.-H. Qu and H. Tian, *Asian J. Org. Chem.*, 2015, **4**, 212; (*b*) J.-N. Zhang, H. Li, W. Zhou, S.-L. Yu, D.-H. Qu and H. Tian, *Chem. – Eur. J.*, 2013, **19**, 17192.
33 H. Zhang, Q. Liu, J. Li and D.-H. Qu, *Org. Lett.*, 2013, **15**, 338.
34 C. M. Álvarez, H. Barbero and D. Miguel, *Eur. J. Org. Chem.*, 2015, 6631.
35 (*a*) V. Blanco, D. A. Leigh, V. Marcos, J. A. Morales-Serna and A. L. Nussbaumer, *J. Am. Chem. Soc.*, 2014, **136**, 4905; (*b*) V. Blanco, D. A. Leigh, U. Lewandowska, B. Lewandowski and V. Marcos, *J. Am. Chem. Soc.*, 2014, **136**, 15775; (*c*) V. Blanco, D. A. Leigh and V. Marcos, *Chem. Soc. Rev.*, 2015, **44**, 5341; (*d*) K. Eichstaedt, J. Jaramillo-Garcia, D. A. Leigh, V. Marcos, S. Pisano and T. A. Singleton, *J. Am. Chem. Soc.*, 2017, **139**, 9376.
36 S. J. Loeb and J. A. Wisner, *Angew. Chem., Int. Ed.*, 1998, **37**, 2838.
37 (*a*) A. M. Elizarov, S.-H. Chiu and J. F. Stoddart, *J. Org. Chem.*, 2002, **67**, 9175; (*b*) S. J. Vella, J. Tiburcio and S. J. Loeb, *Chem. Commun.*, 2007, 4752.
38 N. Noujeim, K. Zhu, V. N. Vukotic and S. J. Loeb, *Org. Lett.*, 2012, **14**, 2484.
39 K. Zhu, V. N. Vukotic and S. J. Loeb, *Angew. Chem., Int. Ed.*, 2012, **51**, 2168.
40 K. Zhu, C. A. O'Keefe, V. N. Vukotic, R. W. Schurko and S. J. Loeb, *Nat. Chem.*, 2015, **7**, 514.
41 K. Zhu, V. N. Vukotic and S. J. Loeb, *Chem. – Asian J.*, 2016, **11**, 3258.
42 C. M. Keaveney and D. A. Leigh, *Angew. Chem., Int. Ed.*, 2004, **43**, 1222.
43 J. D. Crowley, D. A. Leigh, P. J. Lusby, R. T. McBurney, L.-E. Perret-Aebi, C. Petzold, A. M. Z. Slawin and M. D. Symes, *J. Am. Chem. Soc.*, 2007, **129**, 15085.
44 D. A. Leigh, P. J. Lusby, R. T. McBurney and M. D. Symes, *Chem. Commun.*, 2010, **46**, 2382.
45 D. A. Leigh and A. R. Thomson, *Org. Lett.*, 2006, **8**, 5377.
46 (*a*) H. Zheng, W. Zhou, J. Lv, X. Yin, Y. Li, H. Liu and Y. Li, *Chem. – Eur. J.*, 2009, **15**, 13253; (*b*) Y. Zhao, Y. Li, S.-W. Lai, J. Yang, C. Liu, H. Liu, C.-M. Che and Y. Li, *Org. Biomol. Chem.*, 2011, **9**, 7500.
47 S.-Y. Hsueh, C.-T. Kuo, T.-W. Lu, C.-C. Lai, Y.-H. Liu, H.-F. Hsu, S.-M. Peng, C.-h. Chen and S.-H. Chiu, *Angew. Chem., Int. Ed.*, 2010, **49**, 9170.
48 L. Liu, Y. Liu, P. Liu, J. Wu, Y. Guan, X. Hu, C. Lin, Y. Yang, X. Sun, J. Ma and L. Wang, *Chem. Sci.*, 2013, **4**, 1701.
49 B. Hesseler, M. Zindler, R. Herges and U. Lüning, *Eur. J. Org. Chem.*, 2014, 3885.
50 T. Pierro, C. Gaeta, C. Talotta, A. Casapullo and P. Neri, *Org. Lett.*, 2011, **13**, 2650.
51 C. Talotta, C. Gaeta and P. Neri, *Org. Lett.*, 2012, **14**, 3104.
52 J.-S. Cui, Q.-K. Ba, H. Ke, A. Valkonen, K. Rissanen and W. Jiang, *Angew. Chem., Int. Ed.*, 2018, **57**, 7809.
53 D. B. Amabilino, C. O. Dietrich-Buchecker, A. Livoreil, L. Pérez-García, J.-P. Sauvage and J. F. Stoddart, *J. Am. Chem. Soc.*, 1996, **118**, 3905.
54 S. Grunder, P. L. McGrier, A. C. Whalley, M. M. Boyle, C. Stern and J. F. Stoddart, *J. Am. Chem. Soc.*, 2013, **135**, 17691.
55 M. Juríček, J. C. Barnes, N. L. Strutt, N. A. Vermeulen, K. C. Ghooray, E. J. Dale, P. R. McGonigal, A. K. Blackburn, A.-J. Avestro and J. F. Stoddart, *Chem. Sci.*, 2014, **5**, 2724.
56 R. G. Coumans, J. A. Elemans, A. E. Rowan and R. J. Nolte, *Chem. – Eur. J.*, 2013, **19**, 7758.
57 D. A. Leigh, P. J. Lusby, A. M. Z. Slawin and D. B. Walker, *Chem. Commun.*, 2005, 4919.
58 K.-Y. Ng, V. Felix, S. M. Santos, N. H. Rees and P. D. Beer, *Chem. Commun.*, 2008, 1281.
59 M. V. Ramakrishnam Raju and H.-C. Lin, *Org. Lett.*, 2014, **16**, 5564.
60 L. Zhang, V. Marcos and D. A. Leigh, *Proc. Natl. Acad. Sci. U. S. A.*, 2018, **115**, 9397.
61 J. D. Badjić, V. Balzani, A. Credi, S. Silvi and J. F. Stoddart, *Science*, 2004, **303**, 1845.
62 M. C. Jiménez, C. D. Buchecker and J. P. Sauvage, *Angew. Chem., Int. Ed.*, 2000, **39**, 3284.
63 (*a*) M. N. Chatterjee, E. R. Kay and D. A. Leigh, *J. Am. Chem. Soc.*, 2006, **128**, 4058; (*b*) V. Serreli, C. F. Lee, E. R. Kay and D. A. Leigh, *Nature*, 2007, **445**, 523.

64 J. D. Badjic, C. M. Ronconi, J. F. Stoddart, V. Balzani, S. Silvi and A. Credi, *J. Am. Chem. Soc.*, 2006, **128**, 1489.
65 C. Fasting, C. A. Schalley, M. Weber, O. Seitz, S. Hecht, B. Koksch, J. Dernedde, C. Graf, E.-W. Knapp and R. Haag, *Angew. Chem., Int. Ed.*, 2012, **51**, 10472.
66 Y. Yamada, M. Okamoto, K. Furukawa, T. Kato and K. Tanaka, *Angew. Chem., Int. Ed.*, 2012, **51**, 709.
67 Z.-J. Zhang, M. Han, H.-Y. Zhang and Y. Liu, *Org. Lett.*, 2013, **15**, 1698.
68 H. Li, X. Li, Y. Wu, H. Ågren and D.-H. Qu, *J. Org. Chem.*, 2014, **79**, 6996.
69 (*a*) P. R. Ashton, I. Baxter, S. J. Cantrill, M. C. Fyfe, P. T. Glink, J. F. Stoddart, A. J. White and D. J. Williams, *Angew. Chem., Int. Ed.*, 1998, **37**, 1294; (*b*) M. C. Jiménez, C. Dietrich-Buchecker and J.-P. Sauvage, *Angew. Chem., Int. Ed.*, 2000, **39**, 3284; (*c*) J. Rotzler and M. Mayor, *Chem. Soc. Rev.*, 2013, **42**, 44.
70 (*a*) A. Goujon, E. Moulin, G. Fuks and N. Giuseppone, *CCS Chem.*, 2019, **1**, 83; (*b*) R. Tao, Q. Zhang, S. Rao, X. Zheng, M. Li and D. Qu, *Sci. China: Chem.*, 2019, **62**, 245.
71 J. Wu, K. C.-F. Leung, D. Benítez, J.-Y. Han, S. J. Cantrill, L. Fang and J. F. Stoddart, *Angew. Chem., Int. Ed.*, 2008, **47**, 7470.
72 (*a*) F. Coutrot, C. Romuald and E. Busseron, *Org. Lett.*, 2008, **10**, 3741; (*b*) C. Romuald, E. Busseron and F. Coutrot, *J. Org. Chem.*, 2010, **75**, 6516; (*c*) P. Waelès, B. Riss-Yaw and F. Coutrot, *Chem. – Eur. J.*, 2016, **22**, 6837.
73 (*a*) L. Fang, M. Hmadeh, J. Wu, M. A. Olson, J. M. Spruell, A. Trabolsi, Y.-W. Yang, M. Elhabiri, A.-M. Albrecht-Gary and J. F. Stoddart, *J. Am. Chem. Soc.*, 2009, **131**, 7126; (*b*) M. Hmadeh, L. Fang, A. Trabolsi, M. Elhabiri, A.-M. Albrecht-Gary and J. F. Stoddart, *J. Mater. Chem.*, 2010, **20**, 3422.
74 P. G. Clark, M. W. Day and R. H. Grubbs, *J. Am. Chem. Soc.*, 2009, **131**, 13631.
75 G. Du, E. Moulin, N. Jouault, E. Buhler and N. Giuseppone, *Angew. Chem., Int. Ed.*, 2012, **51**, 12504.
76 (*a*) A. Wolf, E. Moulin, J.-J. Cid, A. Goujon, G. Du, E. Busseron, G. Fuks and N. Giuseppone, *Chem. Commun.*, 2015, **51**, 4212; (*b*) A. Goujon, G. Du, E. Moulin, G. Fuks, M. Maaloum, E. Buhler and N. Giuseppone, *Angew. Chem., Int. Ed.*, 2016, **55**, 703; (*c*) A. Goujon, G. Mariani, T. Lang, E. Moulin, M. Rawiso, E. Buhler and N. Giuseppone, *J. Am. Chem. Soc.*, 2017, **139**, 4923; (*d*) A. Goujon, T. Lang, G. Mariani, E. Moulin, G. Fuks, J. Raya, E. Buhler and N. Giuseppone, *J. Am. Chem. Soc.*, 2017, **139**, 14825.
77 H. Li, H. Zhang, Q. Zhang, Q.-W. Zhang and D.-H. Qu, *Org. Lett.*, 2012, **14**, 5900.
78 H. Li, J.-N. Zhang, W. Zhou, H. Zhang, Q. Zhang, D.-H. Qu and H. Tian, *Org. Lett.*, 2013, **15**, 3070.
79 H. Li, X. Li, Z.-Q. Cao, D.-H. Qu, H. Ågren and H. Tian, *ACS Appl. Mater. Interfaces*, 2014, **6**, 18921.
80 H. Li, X. Li, H. Ågren and D.-H. Qu, *Org. Lett.*, 2014, **16**, 4940.
81 (*a*) C. Romuald, A. Ardá, C. Clavel, J. Jiménez-Barbero and F. Coutrot, *Chem. Sci.*, 2012, **3**, 1851; (*b*) C. Clavel, C. Romuald, E. Brabet and F. Coutrot, *Chem. – Eur. J.*, 2013, **19**, 2982.
82 Y.-X. Ma, Z. Meng and C.-F. Chen, *Org. Lett.*, 2014, **16**, 1860.
83 Z. Meng and C.-F. Chen, *Chem. Commun.*, 2015, **51**, 8241.
84 Z. Meng, Y. Han, L.-N. Wang, J.-F. Xiang, S.-G. He and C.-F. Chen, *J. Am. Chem. Soc.*, 2015, **137**, 9739.
85 Y. Abe, H. Okamura, K. Nakazono, Y. Koyama, S. Uchida and T. Takata, *Org. Lett.*, 2012, **14**, 4122.
86 N. Zhu, K. Nakazono and T. Takata, *Chem. Commun.*, 2016, **52**, 3647.
87 S. Erbas-Cakmak, S. D. P. Fielden, U. Karaca, D. A. Leigh, C. T. McTernan, D. J. Tetlow and M. R. Wilson, *Science*, 2017, **358**, 340.
88 C. Biagini, S. D. P. Fielden, D. A. Leigh, F. Schaufelberger, S. Di Stefano and D. Thomas, *Angew. Chem., Int. Ed.*, 2019, **58**, 9876.
89 (*a*) J. A. Berrocal, C. Biagini, L. Mandolini and S. Di Stefano, *Angew. Chem., Int. Ed.*, 2016, **55**, 6997; (*b*) C. Biagini, F. Di Pietri, L. Mandolini, O. Lanzalunga and S. Di Stefano, *Chem. – Eur. J.*, 2018, **24**, 10122; (*c*) C. Biagini, S. Albano, R. Caruso, L. Mandolini, J. A. Berrocal and S. Di Stefano, *Chem. Sci.*, 2018, **9**, 181.
90 A. Ghosh, I. Paul, M. Adlung, C. Wickleder and M. Schmittel, *Org. Lett.*, 2018, **20**, 1046.
91 L.-P. Yang, F. Jia, J.-S. Cui, S.-B. Lu and W. Jiang, *Org. Lett.*, 2017, **19**, 2945.
92 Q. Shi and C.-F. Chen, *Org. Lett.*, 2017, **19**, 3175.
93 Q. Shi and C.-F. Chen, *Chem. Sci.*, 2019, **10**, 2529.
94 (*a*) Z.-Q. Cao, Q. Miao, Q. Zhang, H. Li, D.-H. Qu and H. Tian, *Chem. Commun.*, 2015, **51**, 4973; (*b*) Q. Zhang, S.-J. Rao, T. Xie, X. Li, T.-Y. Xu, D.-W. Li, D.-H. Qu, Y.-T. Long and H. Tian, *Chem*, 2018, **4**, 2670.
95 S. Chen, Y. Wang, T. Nie, C. Bao, C. Wang, T. Xu, Q. Lin, D.-H. Qu, X. Gong, Y. Yang, L. Zhu and H. Tian, *J. Am. Chem. Soc.*, 2018, **140**, 17992.
96 (*a*) H. Meng, M. Xue, T. Xia, Y.-L. Zhao, F. Tamanoi, J. F. Stoddart, J. I. Zink and A. E. Nel, *J. Am. Chem. Soc.*, 2010, **132**, 12690; (*b*) Q. Duan, Y. Cao, Y. Li, X. Hu, T. Xiao, C. Lin, Y. Pan and L. Wang, *J. Am. Chem. Soc.*, 2013, **135**, 10542.

